



Catalyst Deactivation during One-step Dimethyl Ether Synthesis from Synthesis Gas

Journal:	<i>Catalysis Letters</i>
Manuscript ID	CATLET-2016-0434.R1
Manuscript Type:	Original Manuscript
Date Submitted by the Author:	06-Sep-2016
Complete List of Authors:	Dadgar, Farbod; NORWEGIAN UNIVERSITY OF SCIENCE AND TECHNOLOGY, Department of Chemical Engineering Myrstad, Rune; SINTEF, Materials and Chemistry Pfeifer, Peter; Karlsruhe Institute of Technology, Institute for Micro Process Engineering (IMVT) Holmen, Anders; NORWEGIAN UNIVERSITY OF SCIENCE AND TECHNOLOGY, Department of Chemical Engineering Venvik, Hilde; NORWEGIAN UNIVERSITY OF SCIENCE AND TECHNOLOGY, Department of Chemical Engineering
Keywords:	Heterogeneous catalysis < Catalysis, Deactivation < Elementary Kinetics, Acid catalysis < Processes and Reactions, CO hydrogenation < Processes and Reactions, Dehydration < Processes and Reactions, DME < Processes and Reactions, Bifunctionality < Elementary Kinetics
<p>Note: The following files were submitted by the author for peer review, but cannot be converted to PDF. You must view these files (e.g. movies) online.</p>	
<p>Dadgar-2016.tex 01_Introduction.tex 02_Experimental.tex 03_ResultsAndDiscussion.tex 04_Conclusion.tex Farbod-Main-Ref-File.bib model1-num-names.bst</p>	

SCHOLARONE™
Manuscripts

Catalyst Deactivation during One-step Dimethyl Ether Synthesis from Synthesis Gas

Farbod Dadgar^a, Rune Myrstad^b, Peter Pfeifer^c, Anders Holmen^a, Hilde J. Venvik^{a,*}

^a*Department of Chemical Engineering, Norwegian University of Science and Technology (NTNU), NO-7491 Trondheim, Norway*

^b*SINTEF Materials and Chemistry, N-7465 Trondheim, Norway*

^c*Karlsruhe Institute of Technology (KIT), Institute for Micro Process Engineering (IMVT), Hermann-von-Helmholtz-Platz, DE-76344 Eggenstein-Leopoldshafen, Germany*

Abstract

Catalysts for direct synthesis of dimethyl ether (DME) from synthesis gas should essentially contain two functions, i.e. methanol synthesis and methanol dehydration. In the present work, the deactivation of both functions of hybrid catalysts during direct DME synthesis under industrially relevant conditions has been investigated with special focus on the influence of each reaction step on the deactivation of the catalyst function corresponding to the other step. A physical mixture of a Cu-Zn-based methanol synthesis catalyst and a ZSM-5 methanol dehydration catalyst was used. The metallic catalyst appears to deactivate due to Cu sintering, with no apparent effect from the methanol dehydration step under the conditions applied. The acid catalyst deactivates due to accumulation of hydrocarbon species formed in its pores. Synthesis gas composition, i.e. H₂/CO ratio and CO₂-content (which directly affects partial pressure of water), seems to influence the zeolite deactivation.

*Corresponding author.

Email address: hilde.j.venvik@ntnu.no (Hilde J. Venvik)

Preprint submitted to Unknown Journal

April 13, 2016

1
2
3
4
5
6
7
8 *Keywords:*

9
10 DME, methanol synthesis, methanol dehydration, deactivation, hybrid
11 catalyst, H-ZSM-5, Cu/ZnO/Al₂O₃
12
13

14 15 **1. Introduction**

16
17
18 Dimethyl ether (DME) is a colorless, non-toxic gas that can be liquefied
19 under moderate pressures. Earlier, DME was primarily used as an aerosol
20 propellant, but its application has considerably grown over the recent decades
21 as an LPG substitute or for LPG blending, especially in Asia [1–3]. DME
22 is a fuel with high cetane number and clean burning properties that has
23 the potential to replace diesel for use in compression ignition engines after
24 implementation of slight modifications in the fuel injection system [4, 5]. To-
25 day, DME is mainly produced through a conventional two-step route, i.e.
26 methanol synthesis from synthesis gas (mixture of H₂, CO and very often
27 CO₂) over a Cu-Zn-based catalyst, followed by dehydration of methanol to
28 DME over a solid acid catalyst. Alternatively, DME can be produced di-
29 rectly from synthesis gas over a hybrid catalyst capable of catalyzing both
30 methanol synthesis and dehydration in a single step [6, 7]. The direct DME
31 synthesis route is thermodynamically more favorable since syngas conversion
32 to methanol is largely limited by thermodynamic equilibrium and further in
33 situ conversion of methanol to DME shifts this equilibrium towards more
34 methanol formation and allows for higher single-pass conversion of syngas.
35
36
37
38
39
40
41
42
43
44
45
46
47
48

49 Catalyst deactivation is an important aspect of any catalytic process. De-
50 activation of the hybrid direct DME synthesis catalysts may have its roots
51 in deactivation of the methanol synthesis catalyst, the methanol dehydra-
52
53
54
55

1
2
3
4
5
6
7
8
9
10
11
12
13
14
15
16
17
18
19
20
21
22
23
24
25
26
27
28
29
30
31
32
33
34
35
36
37
38
39
40
41
42
43
44
45
46
47
48
49
50
51
52
53
54
55
56
57
58
59
60

tion catalyst or both, and may be caused by the well-known deactivation mechanisms corresponding to each reaction step or by specific deactivation modes originating from interactions between the two catalysts or the distinct reaction environment created by combining the two reaction steps in a single unit.

Methanol synthesis is a well-developed technology and despite the fact that catalyst deactivation has received less attention compared to other aspects of the process, there are still numerous theoretical and experimental studies concerning the matter, which have been extensively reviewed by several authors including Chinchén et al. [8], Kung [9], Twigg and Spencer [10, 11], and Bøggild-Hansen and Højlund-Nielsen [12]. During the first several decades of industrial-scale methanol production, with coal-derived synthesis gas as the feed, poisoning used to be the main concern regarding catalyst deactivation. Sulfur compounds, halogens and especially chlorine, transition metals such as Fe and Ni, alkali metals such as K and Cs, and arsine were identified as poisons for methanol synthesis catalysts [8–12]. The shift from coal to natural gas as the main source of synthesis gas in 1960s, along with improvements with regard to catalyst formulation, enabled the use of more active (but also more sensitive) Cu-based catalysts for methanol synthesis. Today, thanks to the advanced and efficient gas purification technologies, thermal sintering of copper is practically the only important mode of deactivation under normal operation in large-scale plants [10, 11]. The mechanism of thermal deactivation is a subject of an ongoing debate [13–15] and recent findings [16] suggests that additional mechanisms, e.g. disruption of the Cu-Zn synergy, may also play a role in catalyst deactivation. In order to

1
2
3
4
5
6
7
8 restrict the thermal deactivation, methanol synthesis is barely conducted at
9 temperatures higher than or close to 300°C.

10
11 γ -alumina together with zeolites, especially ZSM-5, are the most widely
12 applied solid acid catalysts for methanol dehydration to DME. Alumina is a
13 rather stable catalyst but loses its activity very fast in the presence of H₂O,
14 because of competitive water adsorption on the Lewis acid sites active for
15 methanol dehydration [17–20]. Consequently, γ -alumina may not be suitable
16 for conditions where the partial pressure of water is high, such as the use
17 of crude methanol as the feed or for direct DME synthesis from CO₂-rich
18 synthesis gas. In comparison, the activity of zeolites for methanol dehydra-
19 tion to DME is typically much higher and less susceptible to water inhibition
20 [17, 18]. Zeolites, especially ZSM-5 and SAPO-34, are well-known catalysts
21 for methanol conversion to hydrocarbons (MTH), and have been applied
22 commercially in methanol-to-gasoline (MTG), -olefin (MTO) and -propylene
23 (MTP) processes, where DME forms as an intermediate/byproduct in equi-
24 librium with the methanol feed [21]. Methanol dehydration to DME over
25 zeolites does not require the high temperature (> 350°C) and long contact
26 time which are essential for substantial hydrocarbon yield [22, 23].

27
28 Under typical MTH reaction conditions, coking is the well-known cause
29 of zeolite deactivation [24]. Despite the wealth of information on deactiva-
30 tion under such conditions, in-depth investigation of H-ZSM-5 deactivation
31 during DME synthesis, i.e. methanol dehydration under lower T and shorter
32 contact time required to obtain high DME selectivity [23], is rather scarce.
33 Nevertheless, investigations of the MTH reaction at low temperatures (260-
34 300°C) by Schulz et al. [25–32] have provided valuable insights into the de-
35
36
37
38
39
40
41
42
43
44
45
46
47
48
49
50
51
52
53
54
55
56
57
58
59
60

1
2
3
4
5
6
7
8 activation mechanism of ZSM-5 during DME formation. According to their
9 results, conversion of methanol/DME to hydrocarbons over ZSM-5 begins
10 at a low rate with formation of unsaturated hydrocarbons, mainly retained
11 inside catalyst pores, and co-production of methane. Subsequently, fast re-
12 actions of methanol with the retained hydrocarbons and the hydrocarbons
13 with each other, intensify the hydrocarbon formation rate autocatalytically.
14 Highly alkylated mono-ring arenes, especially ethyl-trimethyl-benzene and
15 isopropyl-dimethyl-benzene, are the largest molecules that can form inside
16 ZSM-5 pore system (channel intersections 9.4 Å) through alkylation of the
17 benzene ring with light olefins, as demonstrated in Fig. 1. However, they are
18 too big to diffuse out of the pores (channel openings of 5.1-5.6 Å). At high
19 temperatures, benzene ring alkylation is reversible and the bulky alkylated
20 benzene molecules break to smaller aromatics and olefins that can diffuse out
21 of the ZSM-5 pores, but below 400°C, these molecules are rather stable and
22 eventually deactivate ZSM-5 by filling the pores. Growth of hydrocarbons
23 beyond bulky monocyclic arenes inside ZSM-5 pores is strongly restricted
24 by spatial constraints, therefore, coke may only form on the outer surface of
25 the ZSM-5 crystals [22, 30]. ZSM-5, owing to its three-dimensional 10-ring
26 structure without trapping cavities, is much more resistant towards deacti-
27 vation by coke compared to large pore zeolites with e.g. BEA, AFI, and CHA
28 structures [18, 21]. Coking is favored by high temperatures (> 400°C) and
29 long contact times, and extensive coke formation can eventually deactivate
30 the catalyst by blocking pore openings.
31
32
33
34
35
36
37
38
39
40
41
42
43
44
45
46
47
48
49

50 During direct DME synthesis, deactivation of methanol synthesis and
51 methanol dehydration catalysts through the aforementioned mechanisms could
52
53
54
55

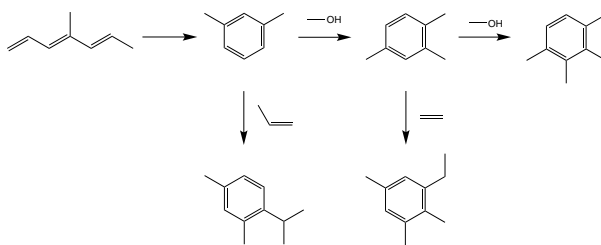


Figure 1: Irreversible alkylation of monocyclic aromatics leading to pore filling, proposed by Schulz et al. [31, 32] as the mechanism of ZSM-5 deactivation during methanol conversion at low temperature.

be affected by the distinct reaction atmosphere created by combining the two reactions. For instance, water and methanol are involved in both reaction steps and their concentrations in the reaction medium may differ from those of each separate step under otherwise similar conditions (T, P). Steam produces diverse effects on both functions of the catalyst, e.g. enhances the stability of Cu-Zn-based catalysts in low concentrations [33], assists Cu sintering [33–37] and disruption of the Cu-Zn synergy [16] at high partial pressures, hinders coke formation [20], deactivates γ - Al_2O_3 by strong adsorption [17–19], and reduces formation of deactivating carbonaceous compounds on H-ZSM-5 [18]. High partial pressure of methanol is also suggested to intensify Cu sintering [38]. Moreover, certain dehydration byproducts such as toluene, if present in large concentrations (500 ppm), can permanently deactivate the Cu-based catalyst through wax formation and pore filling [39]. Limited learning also exists from the literature concerning the effect of synthesis gas compositions on deactivation of the solid acid catalyst [40, 41].

Detrimental interactions between Cu-Zn-based methanol synthesis function and γ - Al_2O_3 [42] or ZSM-5 [37, 43–47] methanol dehydration function

1
2
3
4
5
6
7
8 have also been identified as a possible cause of deactivation. García-Trenco
9 and Martínez reported a correlation between the concentration of extra-
10 framework Al species (EFAl) on the ZSM-5 surface and deactivation of the
11 hybrid catalyst, and concluded that the EFAl species may migrate onto the
12 metallic catalyst through a water assisted mechanism, thereby disrupting the
13 Cu-Zn synergy [45, 46]. On the other hand, García-Trenco et al. also sug-
14 gested that Cu-Zn-based methanol synthesis catalyst contributes to ZSM-5
15 deactivation through partial blockage of zeolite pores as well as ion exchange
16 of acidic H⁺ by Cu²⁺ (and possibly also Zn²⁺) [43]. Similarly, Ordonsky et al.
17 contended that migration of Cu into the zeolite pores through a mechanism
18 assisted by water and hydroxyls (Brønsted acid sites) on the outer surface
19 of ZSM-5, and subsequent ion exchange between Cu²⁺ and acidic H⁺ of the
20 zeolite, deactivate both functions of the hybrid catalyst [37]. Peng et al.
21 investigated the deactivation of a hybrid catalyst composed of a commercial
22 methanol synthesis catalyst and γ -Al₂O₃ and suggested the migration of Cu-
23 and Zn-containing species from the metallic to the acid catalyst as a cause
24 of deactivation of both functions [42]. The preparation method of the hybrid
25 catalyst is central to this deactivation mechanism as intimate solid-state con-
26 tact between the two catalysts is necessary for such interactions to take place
27 [37, 42–45]. According to the results reported by García-Trenco et al. [43–45],
28 intimate contact of the two catalyst components does not seem to provide
29 any enhancement in the catalytic performance, hence, in this study a mix-
30 ture of pre-pelletized catalysts were used to prevent the adverse interactions
31 between the two components.
32
33
34
35
36
37
38
39
40
41
42
43
44
45
46
47
48
49
50
51

52 The objective of the present work is to investigate catalyst deactiva-
53
54
55

tion during direct DME synthesis, with more focus on interactions between methanol formation and methanol dehydration. Cu-Zn-based methanol synthesis catalyst and ZSM-5 methanol dehydration catalyst were studied, first, under conditions corresponding to each reaction step and then under direct DME synthesis conditions. The operating conditions were chosen to be as representative of typical industrial conditions as possible, which is not always the case in the literature due to practical challenges involved with high methanol partial pressures. The common ambiguity in the literature regarding which reaction step controls the overall DME synthesis kinetics, was avoided.

2. Experimental

2.1. Catalysts and catalysts characterization

Two different commercial Cu/ZnO-based and one homemade Cu/ZnO/Al₂O₃ methanol synthesis catalysts were used throughout this study, which are referred to as CZ-C1, CZ-C2 and CZ-H, respectively. The homemade catalyst was prepared by conventional co-precipitation, where an aqueous solution of Cu(NO₃)₂, Zn(NO₃)₂ and Al(NO₃)₃ was precipitated with a sodium carbonate solution, through slowly adding the two to an aqueous solution of sodium acetate at 50°C and pH of 7. The precipitates were then aged for 30 min, washed extensively with deionized water, dried over night at 120°C and calcined at 400°C for 2 h under flow of air. Prior to calcination, the Na-content of the precipitates was checked using ICP-MS and confirmed as below 90 ppm. ICP-MS also indicated the Cu/Zn/Al molar ratio of the resultant catalyst as 22/57/21 mol.%. Prior to introduction of synthesis gas,

1
2
3
4
5
6
7
8 CZ catalysts were reduced in situ under a flow of 3% H₂ in N₂ over a 9 h-long
9 stepwise temperature increase, followed by 8 h dwell at 250°C.

10
11 The H-ZSM-5 methanol dehydration catalyst was prepared by calcination
12 of NH₄-ZSM-5 (CBV 8014, Zeolyst Int., SiO₂/Al₂O₃=80) at 600°C for 4 h.
13 The acidity of the zeolite was manipulated through proton-sodium exchange
14 by treating an aliquot of the H-ZSM-5 with a NaNO₃ 0.05 M solution at
15 80°C, followed by washing with deionized water, overnight drying at 100°C
16 and calcining at 600°C for 4 h. The Na/Al atomic ratio of the NaH-ZSM-5
17 was 0.12 as determined by ICP-MS and the acidity was 10% lower than the
18 parent zeolite as measured by NH₃-TPD. Hybrid catalysts for direct synthesis
19 of DME were prepared by physically mixing the dry pre-pelletized metallic
20 and acid catalysts in a 8-to-1 ratio (mass based). For the sake of comparison,
21 γ -alumina (PURALOX 5/200 from Sasol Germany) was also used in a few
22 experiments as the dehydration function of the hybrid catalyst in an Al/CZ
23 ratio of 2. All catalysts were used as powders in a particle size range of 80-
24 125 μ m. The methanol dehydration experiments were performed over zeolite
25 diluted with α -alumina, which was prepared by treating PURALOX 5/200
26 at 1150°C overnight. The structural change from γ to α -Al₂O₃ was confirmed
27 by XRD.
28
29
30
31
32
33
34
35
36
37
38
39
40
41
42

43 Fresh and used catalysts (except for CZ-C1 and -C2) were characterized
44 by various techniques. The BET surface area was estimated from the ni-
45 trogen desorption isotherm at 77K, measured using a Micromeritics TriStar
46 3000. Samples were outgassed overnight under 0.05 mbar pressure at 200°C
47 prior to the measurements. Powder X-ray diffraction (XRD) analyses were
48 done using a Bruker D8 Focus powder diffractometer equipped with a Lynx-
49
50
51
52
53
54
55
56
57
58
59
60

1
2
3
4
5
6
7
8 Eye™ detector, using Cu K α radiation. The samples were analyzed between
9 the 2θ angles of 15° and 80°, and the diffraction data were analyzed us-
10 ing the Bruker DIFFRACplus EVA software. Present phases were identified
11 by a search/match procedure using the 2009 edition of the ICDD PDF4+
12 database. In addition, the Bruker DIFFRACplus TOPAS software was used
13 for quantitative phase analyses (Cu crystallites size by applying the Scher-
14 rer equation on Cu(111) peaks). X-ray photoelectron spectroscopy (XPS)
15 was applied to detect possible accumulation of carbon, Fe or Ni on the cat-
16 alyst surface after experiments and identify the oxidation state of Cu and
17 Zn. An Axis UltraDLD XP spectrometer from Kratos Analytical was used
18 and selected catalyst samples were analyzed using both monochromatic Al
19 K α and achromatic Mg K α X-ray sources. Samples were outgassed under
20 $10^{-8} - 3 \times 10^{-9}$ Torr pressure in the analysis chamber. Elemental analysis of
21 the catalysts was done using a Thermo Scientific Element 2 high resolution
22 ICP-MS. Powdered ZSM-5 and CZ samples were mixed with, respectively, a
23 concentrated HNO₃-HF mixture and a 50% v/v HNO₃ solution, digested in
24 an ultrasonic bath at 80°C and then diluted prior to analysis. The acidity
25 of the zeolite samples were measured by NH₃-TPD method in a NETZSCH
26 STA 449C thermo-microbalance coupled with a QMS 403C mass spectrom-
27 eter. The samples were pre-treated in situ at 600°C for 1 h, prior to adsorp-
28 tion taking place at 100°C under a gas flow composed of 1% NH₃ in Ar for
29 30 min. Samples were then purged with Ar for 1.5 h at 100°C before thermal
30 desorption spectra being recorded by increasing the temperature from 100 to
31 800°C. Thermal and oxidative treatment of deactivated zeolite samples were
32 also performed in the same instrument. TPD spectra were obtained between
33
34
35
36
37
38
39
40
41
42
43
44
45
46
47
48
49
50
51
52
53
54
55
56
57
58
59
60

1
2
3
4
5
6
7
8 200 and 600°C under Ar flow, after a 40 min in situ pre-treatment at 200°C.
9
10 Subsequently, the samples were exposed to oxygen by substituting argon flow
11
12 with air at 600°C.
13

14 *2.2. Reactor and experimental setup*

15
16 The methanol dehydration experiments were conducted in an isother-
17 mal stainless steel tubular fixed-bed reactor (ID=9 mm). The reactor was
18 clamped in between two half-cylindrical aluminum blocks to ensure a uniform
19 heat transfer, and placed in a Kantal oven equipped with a Eurotherm tem-
20 perature controller. Temperature was monitored in the catalyst bed (~1 cm)
21 by moving the thermocouple along a thermowell installed along the axis of
22 the reactor. To keep the reaction temperature fully under control, the highly
23 exothermic methanol and direct DME syntheses experiments were conducted
24 in a stainless steel fixed-bed microstructured reactor-heat exchanger, fabri-
25 cated in Karlsruhe Institute of Technology, Germany. The reactor consists of
26 a 6 cm-long reaction slit with rectangular cross section of 8.8 mm×1.5 mm,
27 sandwiched between cross flow channels for circulation of heat transfer oil.
28 The reaction temperature was monitored by inserting several thermocouples
29 into the dedicated holes on top of the reactor housing along its center line,
30 which provides proximity (~2 mm) to the catalyst bed. The pressure drop
31 of the catalyst bed was measured before and after each experiment using a
32 pressure transducer to confirm insignificant changes in catalyst packing. The
33 micro-structured reactor has been thoroughly studied earlier in our group for
34 methanol [48–50], direct DME [51–53] and Fischer-Tropsch [54] syntheses,
35 and has been established as practically isothermal, isobaric and free from
36 mass transfer limitations under conditions similar to the ones applied in the
37
38
39
40
41
42
43
44
45
46
47
48
49
50
51
52
53
54
55
56
57
58
59
60

present study.

Premixed synthesis and carrier gases were of 5.0 quality (99.999% purity) or higher. Compositions of the gases used are summarized in Table 1. The gases were fed through digital mass flow controllers (Bronkhorst), and pressure was controlled using a digital back pressure controller (Bronkhorst). Introduction of methanol or water was done by evaporating the pressurized liquid into the feed gas stream using a Controlled Evaporator Mixer (Bronkhorst). To investigate the effect of impurities on deactivation, pulses of xylene was injected into the feed, by first evaporating ~ 1 g xylene in a small sample cylinder and then redirecting the feed flow to pass through the container. Feed and product tubing was heated to $\sim 180^\circ\text{C}$ to eliminate temperature gradient at the catalyst bed inlet and prevent condensation of water, methanol and trace concentrations of other possible liquid products. The products were analyzed online using an Agilent 7890 gas chromatograph, equipped with a thermal conductivity and flame ionization detectors. Nitrogen and CH_4 were used as internal standards to perform the calculations. The carbon mass balance over the system closes within 5% or smaller (often below 3%) error margin at all times. The error is caused partly by not quantifying the hydrocarbon byproducts of methanol dehydration. Blank tests confirmed inactivity of the setup and α -alumina dilutant.

3. Results and discussion

3.1. Deactivation of methanol synthesis catalyst

Fig. 2 presents an example of the activity loss during methanol synthesis, both as a drop in normalized methanol formation rates (left axis) and as a

Table 1: Compositions (mol%) of the applied synthesis and carrier gases.

	H ₂	CO	CO ₂	CH ₄	N ₂
Syngas-1	42	42	5	6	5
Syngas-2	56	28	5	6	5
CGas-1	0	0	0	5	95
CGas-2	42	0	0	3.4	64.6
CGas-3	0	42	0	3.4	64.6

reduction in absolute CO conversion values (right axis). Comparable levels of deactivation were observed for all methanol synthesis catalysts under similar operating conditions. Fig. 2 also clearly shows the importance of monitoring catalyst deactivation at low conversion levels, as the data measured at a lower space velocity (resulting in higher conversion) suggests a considerably lower deactivation due to the effect of equilibrium on the syngas conversion.

Pure premixed synthesis gas was used for the experiments (impurity level below 10 ppm) and common poisons such as S and Cl were not present in any of the raw materials used. Iron and nickel carbonyls, however, could in theory form inside the reactor, tubing or gas cylinders (if the internal surface is not coated with aluminum) from steel in contact with syngas. For this reason, a carbonyl trap containing PbO was installed upstream of the reactor. According to the ICP-MS analysis, fresh CZ-H catalyst contains 21 and 2 ppmw of Fe and Ni, respectively. The XPS analyses show negligible amounts of iron and nickel (less than 0.4 mol% total) on the surface of different fresh and used CZ-H catalyst samples, without any obvious trend of concentration change after the reaction experiments. Moreover, XPS confirms no accumulation of

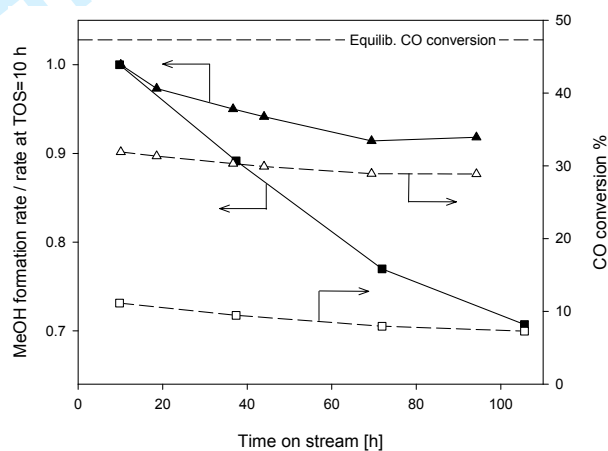


Figure 2: Deactivation of CZ-C2 catalyst during methanol synthesis from Syngas-2, as measured at 250°C, 50 bar and either space velocity of 250 (▲/△) or 800 Ncm³/min/g_{cat.} (■/□). Solid lines show normalized methanol formation rates on the left axis and dash lines show CO conversions on the right axis. Equilibrium CO conversion is estimated from the Gibbs free energy of the compounds using Aspen HYSYS V8.0 software.

1
2
3
4
5
6
7
8 carbon on the catalyst surface even after more than 200 h on stream time.
9
10 An increase in the surface concentration of carbon could have been a sign of
11 either Fischer-Tropsch activity and wax formation related to the presence of
12 Fe, or less likely, coke deposition on the catalyst as claimed to be happening
13 by Sierra et al. [20, 55–58]. Changes in the BET surface area of the catalyst
14 do not follow any particular pattern and hence, do not provide any informa-
15 tion with regard to the catalyst deactivation. The N₂ adsorption analyses
16 of catalysts before and after catalysis indicated a slight increase in the BET
17 surface area of the CZ-H catalyst from ~63 to 70–75 m²/g_{catal.}, while showed
18 a slight decrease for CZ-C1 catalysts in a similar range.
19
20
21
22
23
24
25

26
27 Copper sintering is known as the main cause of Cu/ZnO-based catalyst
28 deactivation in the absence of poisons [10–12]. Fig. 3 demonstrates the X-ray
29 diffraction patterns of a fresh, freshly reduced and used samples of the CZ-
30 H catalyst. For the fresh sample, only CuO and ZnO peaks are detectable
31 in the diffractogram. Diffraction pattern of the reduced sample confirms
32 the reduction of crystalline CuO to copper crystallites of an average size of
33 5.3 nm. After being on stream for more than 100 h, average Cu crystallite
34 size of the catalyst grew to 7.8 nm. This can be an indication of Cu sintering.
35 However, it should be noted that ex situ XRD measurements have limitations
36 with regard to possible oxidation of copper upon exposure of the reduced
37 catalyst to the atmosphere as well as the fact that it does not provide direct
38 information regarding the active surface area of the catalyst [59].
39
40
41
42
43
44
45
46
47
48

49 Catalyst deactivates slightly faster under Syngas-1 containing 42% CO,
50 than under Syngas-2 with 28% CO. This is in agreement with the reported
51 experimental results suggesting a correlation between the deactivation and
52
53
54
55

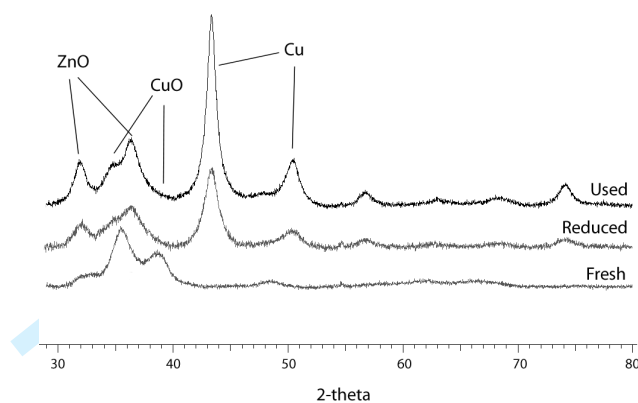


Figure 3: X-ray diffraction patterns of CZ-H in three different states; fresh, reduced and used (operated for 104 h at 210-270°C). Positions of the main peaks correspond to the detected crystalline phases are indicated on the diffractogram.

the CO pressure [35, 60, 61], and the key role of CuCO as the mobile Cu specie in sintering and deactivation of the catalyst, suggested by Rasmussen et al. [13] based on density functional theory (DFT) calculations. The homemade catalyst (CZ-H) is slightly more stable than the commercial catalysts under identical conditions, although much less active. This can be linked to a likely considerably lower Cu content of the CZ-H, and higher ZnO content that acts as spacers between the Cu nanocrystals, suppressing their sintering. According to the ICP-MS analysis the CuO/ZnO/Al₂O₃ molar ratio of the CZ-H is 25/65/10, as opposed to ~60/30/10 mol% expected for the typical commercial methanol synthesis catalysts [62].

Ruling out all other known causes of CZ catalyst deactivation, the growth of Cu crystallite seems to be the sole cause of the observed activity loss. Nevertheless, all CZ catalysts showed rather good stability, considering the harsh operating conditions they were exposed to. This could partly have its

1
2
3
4
5
6
7
8 roots in the enhanced heat transfer characteristics of the micro structured
9 reactor used, which provides a practically isothermal profile throughout the
10 catalyst bed [50, 51]

11
12
13
14 It is worth mentioning that the Cu-Zn is a dynamic system and the copper
15 crystallites shape, and hence the catalyst activity, changes reversibly upon
16 alteration of the reaction medium composition [63]. Transient kinetic data
17 indicated that stabilization of the catalyst surface and its activity after a
18 change in gas composition may take up to several hours [41, 64]. In our
19 experiments, the initial activity is chosen as the activity after 10 h, much
20 longer than what is needed to reach steady-state (overall C balance with
21 less than 5% error), in order to eliminate the effect of syngas introduction
22 (sudden change in the composition) on the activity changes. Nevertheless,
23 such effects may still partly explain a rather larger drop in the methanol
24 formation rate at the beginning of some experiments.
25
26
27
28
29
30
31
32
33
34

35 *3.2. Deactivation of ZSM-5*

36
37 Fig. 4 demonstrates ZSM-5 deactivation during methanol dehydration to
38 DME at 250°C under a methanol partial pressure of 1.5 bar (for the sake
39 of comparison, equilibrium conversion of Syngas-1 at 250°C and 50 bar re-
40 sults in $P_{\text{MeOH}} \sim 7$ bar at the methanol reactor outlet). At the conditions
41 applied, the initial methanol conversion was around 75% (as opposed to an
42 equilibrium conversion of 88%) and the selectivity towards DME was above
43 95%. Formation of trace amounts of various hydrocarbons/oxygenates was
44 detected with the GC's flame ionization detector, although identification and
45 quantification of these byproducts were not performed. The color of severely
46 deactivated H-ZSM-5 samples changed from white to yellowish brown. Such
47
48
49
50
51
52
53
54
55
56
57
58
59
60

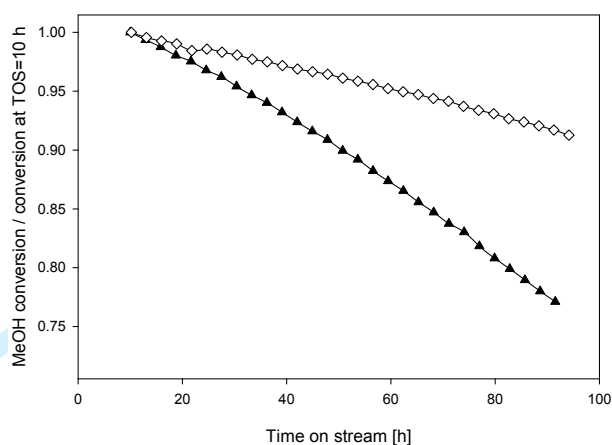


Figure 4: Deactivation of H-ZSM-5 (▲) and NaH-ZSM-5 (◇) during methanol dehydration to DME at 250°C, $P_{\text{total}}=10$ bar, $P_{\text{MeOH}}=1.5$ bar, using CGas-1 as the carrier gas. Space velocities were chosen respectively as 60 h^{-1} and 40 h^{-1} to yield similar initial methanol conversion level.

color change of the H-ZSM-5 was also reported by Schulz et al. [27, 28, 30] during methanol conversion to hydrocarbons at low temperatures (300°C). They linked the yellow color of the deactivated catalyst to formation and accumulation of highly unsaturated organic compounds at low temperatures, as opposed to the black color of the deactivated H-ZSM-5 during methanol conversion at 450°C, which was explained by coke formation on the outer surface of the catalyst [27, 30]. Measurement of the catalyst surface area with N_2 adsorption before and after the experiments shows a drop in the BET surface area, although no close correlation between the activity loss and the changes in surface area could be drawn. For example, the BET surface area of the deactivated H-ZSM-5 at 58% and 10% of its initial activity were respectively 130 and $123 \text{ m}^2/\text{g}_{\text{catal.}}$, as opposed to $\sim 377 \text{ m}^2/\text{g}_{\text{catal.}}$ for the fresh zeolite.

1
2
3
4
5
6
7
8 To obtain further information regarding the nature of deactivating species,
9 used catalyst samples were subjected to heat treatment under inert atmo-
10 sphere (Ar flow), followed by oxidation at high temperature. An example of
11 the results is presented in Fig. 5. The TPD spectrum was recorded between
12 200-600°C in a thermo-microbalance, after pre-treatment at 200°C to remove
13 species that might be adsorbed on the catalyst after the reaction. The mass
14 reduction of the sample upon heating indicates desorption of species between
15 300 and 400°C, peaking around 320°C. With the small amount of sample that
16 could be accommodated in the sample holder, the compounds desorbed were
17 too diverse and too low in concentration to be detected with good preci-
18 sion using the mass spectrometer coupled with the microbalance. Following
19 the TPD, argon flow was substituted with air at 600°C. Upon introduction
20 of oxygen, a sudden but small reduction in the sample mass was detected
21 along with evolution of CO₂ and water in the effluent, indicative of oxida-
22 tion of remaining adsorbed carbonaceous compounds on the catalyst. These
23 results suggest that the main part of the products retained on the catalyst
24 during methanol dehydration to DME at 230-270°C, decompose/desorb at
25 300-400°C and only a small part is sufficiently stable to remain on the cata-
26 lyst even at temperatures as high as 600°C. This latter part likely has coke
27 like characteristics, and if so, should have been formed on the outer surface
28 of the catalyst since the ZSM-5 pore system strongly prohibits formation of
29 multicyclic aromatic compounds inside the channels [30].

30
31
32
33
34
35
36
37
38
39
40
41
42
43
44
45
46
47
48
49 The results from the thermogravimetric analyses are consistent with the
50 results of a comparable study conducted by Schultz et al. and their sug-
51 gested deactivation mechanism [27, 28, 30–32]. They studied H-ZSM-5 cat-
52
53
54
55

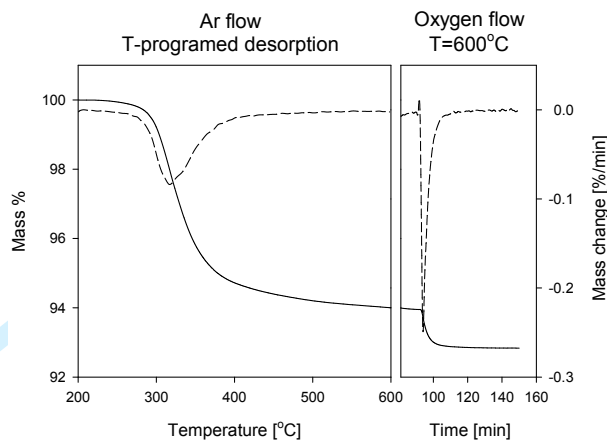


Figure 5: Thermal (left panel) and oxidative (right panel) treatments of H-ZSM-5 deactivated during methanol dehydration at 230-270°C and $SV=7 \text{ h}^{-1}$. Solid and dashed lines shows normalized sample mass and mass changes, respectively.

alysts deactivation during methanol conversion to hydrocarbons (MTH) at low temperatures (270-290°C), using TPD, and reported desorption of retained compounds between 200-400°C with a maximum occurring at around 310°C (increasing slightly with the MTH reaction temperature at which the catalysts were deactivated) [28]. A sophisticated sampling technique was used to enable detailed analysis of the effluent gas during TPD. Results confirmed desorption of a wide range of aromatics, olefins and paraffins from the used catalyst upon heating, with trimethyl benzene and xylene as the dominating aromatics and ethene and propene as the main aliphatic hydrocarbons. Furthermore, their direct analyses of the retained compounds after dissolution of the encapsulating zeolite network in HF and extraction of the organic fraction with a solvent indicated that retained hydrocarbons are mainly composed of multi-alkylated benzene molecules. Consequently,

Schultz et al. concluded that, at low temperatures, H-ZSM-5 deactivates due to formation (and accumulation) of bulky mono-ring arenes inside the zeolite pores through irreversible alkylation of benzene rings with light olefins (see Fig. 1). The alkylation reaction becomes reversible at higher temperatures, allowing deactivating bulky aromatics to escape the zeolite after dealkylation to smaller molecules [25–32].

Along with H-ZSM-5 deactivation, Fig. 4 also presents the deactivation behavior of Na_{12%}H_{88%}-ZSM-5. The ion-exchanged zeolite with acid site density of 1.47 mmol/g_{catal.}, shows almost 10% less acidity in comparison with the parent zeolite (1.63 mmol/g_{catal.}), as measured by NH₃-TPD. Deactivation of the two catalysts was compared under identical conditions, except for different space velocities that were chosen in a way to yield similar level of initial methanol conversion. The zeolite with lower acidity demonstrates a better stability, but as expected, a lower activity. The initial methanol conversion rate over NaH-ZSM-5 was $\sim 287 \mu\text{mol/s/g}_{\text{catal.}}$ as opposed to $\sim 385 \mu\text{mol/s/g}_{\text{catal.}}$ for H-ZSM-5 under the identical conditions specified under Fig. 4. The activity of ZSM-5 for methanol dehydration to DME is usually determined by its Brønsted acid sites, although the contribution of EFAl-related strong Lewis acid sites cannot be ignored completely [17, 44]. Since methanol dehydration to DME does not require strong Brønsted acid sites (unlike methanol conversion to hydrocarbons), partial deactivation of these sites with e.g. sodium or ammonia, or using a zeolite with lower acidity (higher Si/Al ratio) is known to improve DME selectivity and catalyst stability, though at a cost of reduced activity. [18, 65].

Fig. 6 provides some insights into the effect of temperature on H-ZSM-5

1
2
3
4
5
6
7
8 deactivation during methanol dehydration to DME. In comparison to the
9 deactivation rate at 250°C, the catalyst seems to deactivate slower at both
10 higher (290°C) and lower (210°C) temperatures. This observation is in agree-
11 ment with the results reported by Schulz and Wei [28] with regard to H-ZSM-
12 5 deactivation during methanol conversion to hydrocarbons at 260-290°C.
13 According to their study, the rate of hydrocarbon formation (either volatile
14 or retained on the catalyst), and hence, the rate of catalyst deactivation de-
15 creases by lowering the temperature and drops considerably below 270°C. On
16 the other hand, H-ZSM-5 deactivation through pore filling by the retained
17 hydrocarbons decreases as the temperature increases. This is explained as
18 a result of an equilibrium shift towards the reactants in the benzene alkyla-
19 tion reactions, and therefore, dealkylation of the bulky hydrocarbons which
20 are trapped in the zeolite pores to smaller molecules that can diffuse out
21 of the channels. As a result of these two contradicting effects, the maxi-
22 mum deactivation rate was observed at 270-280°C in the temperature range
23 investigated.
24
25
26
27
28
29
30
31
32
33
34
35
36

37
38 Considering the low rate of hydrocarbon formation at low temperature
39 and short contact time relevant for DME production, it is worth stressing
40 that the presence of hydrocarbon impurities, in the feed or on the catalyst,
41 may also play a role in the zeolite deactivation. The MTH reaction follows
42 a hydrocarbon-pool mechanism, and methanol reacts much faster with hy-
43 drocarbons in the pool rather than directly with other methanol molecules
44 [21]. Considerably lower initial conversion rate when highly purified reactant
45 feed and catalysts are used [66] suggests that the direct methanol or DME
46 conversion is of little practical importance even for formation of the "first"
47
48
49
50
51
52
53
54
55

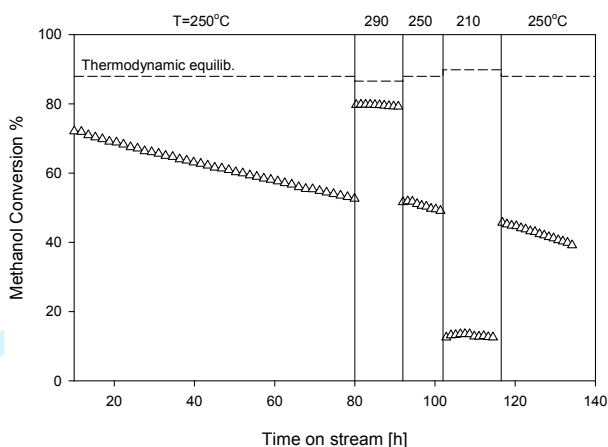


Figure 6: Effect of temperature on deactivation of H-ZSM-5 during methanol dehydration to DME at $P_{\text{total}}=10$ bar, $P_{\text{MeOH}}=1.5$ bar, and $SV=60 \text{ h}^{-1}$ using CGas-3 as the carrier gas. Equilibrium methanol conversion is estimated from the Gibbs free energy of the compounds using Aspen HYSYS V8.0 software.

C-C bonds, since such reactions, if taking place, proceed at a rate so low that they are eclipsed by the reaction of methanol with trace hydrocarbon impurities from various sources. Therefore, the deactivation behavior of the zeolite catalyst during methanol dehydration at low temperatures may be sensitive to the presence of carbonaceous impurities. Nevertheless, no effect on the deactivation trend of the H-ZSM-5 was observed after several injections of xylene to the reactor feed (pulses of ~ 1 g xylene evaporated into the feed stream) during methanol dehydration at 250°C . According to the deactivation mechanism discussed earlier (see Fig. 1), xylene is one of the key intermediates leading to formation of the deactivating species.

For the sake of comparison, the deactivation of γ -alumina was also examined under conditions identical to the ones used for H-ZSM-5 in Fig 4. As expected, the methanol dehydration activity was much lower over $\gamma\text{-Al}_2\text{O}_3$

1
2
3
4
5
6
7
8 (methanol conversion rate of $\sim 106 \mu\text{mol/s/g}_{\text{catal.}}$) in comparison with H-
9 ZSM-5 ($\sim 385 \mu\text{mol/s/g}_{\text{catal.}}$). Alumina experienced a rather dramatic ac-
10 tivity loss (20% drop in methanol conversion) in the first 10 h on stream,
11 probably due to the well-known competitive adsorption of product water on
12 the active sites [17–20]. After TOS of 10 h, deactivation was comparable to
13 the H-ZSM-5 deactivation, although under very different methanol conver-
14 sion levels, 20% as opposed to 75%.

21 22 *3.3. Deactivation of the hybrid catalyst*

23
24 In addition to the aforementioned deactivation modes for CZ and H-ZSM-
25 5 catalysts, it is investigated whether conditions created due to combining
26 methanol synthesis and methanol dehydration in a single unit can affect the
27 deactivation of either components of the hybrid catalyst for direct DME
28 synthesis. The hybrid catalysts were prepared by physically mixing the pre-
29 pelletized CZ catalysts with solid acid catalysts as previously mentioned.

30 31 32 33 34 35 36 37 *3.3.1. Effect of methanol dehydration on CZ deactivation*

38 A possible effect from methanol dehydration on the stability of CZ cata-
39 lyst may originate from the presence of the solid acid catalyst in proximity of
40 the CZ catalyst or the presence of methanol dehydration products, i.e. DME,
41 water or hydrocarbon by-products in the reaction medium. Such effects were
42 investigated earlier in our group as part of a broader study concerning the
43 effects of methanol dehydration on methanol formation reactions [67]. Fig. 7
44 presents the deactivation behavior of the CZ-C2 catalyst along with three
45 different hybrid catalysts composed of a mixture of CZ-C2 with either H-
46 ZSM-5, NaH-ZSM-5 or $\gamma\text{-Al}_2\text{O}_3$ as dehydration components. Deactivation
47
48
49
50
51
52
53
54
55
56
57
58
59
60

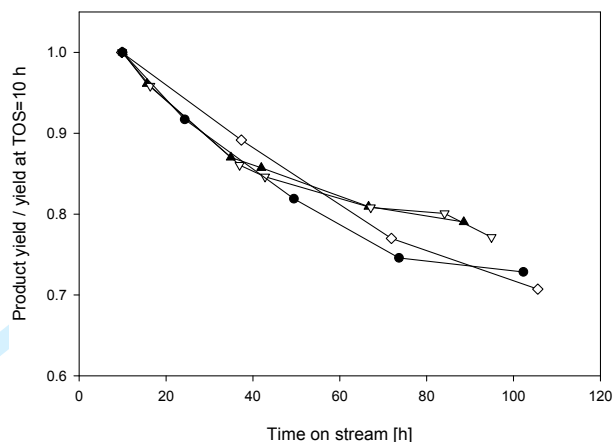


Figure 7: Apparent activity loss of the CZ-C2 catalyst during methanol synthesis (◇) and direct DME synthesis in a hybrid with HZSM-5 (▲), NaHZSM-5 (●), and γ -Al₂O₃ (▽) from Syngas-2. Product yield at T=250°C and P=50 bar is normalized against the yield at TOS=10 h.

was monitored as a normalized product yield under identical conditions, except for a higher space velocity used for the methanol synthesis experiment that was essential to eliminate the effect of thermodynamic equilibrium on the methanol yield observed. The catalysts were subjected to a sequence of changes in reaction conditions (T=210-270°C, P=10-50 bar) between the data points, however the changes were similar with respect to type, timing and quantity for all the runs. All the experiments were kinetically controlled by methanol formation reactions (hybrid catalysts contain an excess of dehydration function) throughout the studied TOS, and the observed declines in the DME/methanol yield are therefore directly related to the loss of methanol formation activity. Fig. 7 indicates no effect from the methanol dehydration products or either of the solid acid catalysts on CZ catalyst deactivation under the condition applied.

1
2
3
4
5
6
7
8 The result is consistent with the experimental results reported by García-
9 Trencó et al. [43–45] confirming no effect from acid catalysts (irrespective of
10 their acidity) on CZ catalyst stability for a hybrid made by mixing pre-
11 pelletized components, as opposed to an enhanced deactivation of the hybrid
12 catalysts prepared by grinding or slurring (in water) the catalyst compo-
13 nents prior to pelletizing. The latter methods are known to create intimate
14 solid-state contact between the two catalysts, which seems essential for detri-
15 mental interactions to take place.
16
17
18
19
20
21
22
23

24 3.3.2. Effect of methanol synthesis on ZSM-5 deactivation

25 The activity of H-ZSM-5 in dehydration of methanol is an order of magni-
26 tude higher than the CZ activity for methanol synthesis based on the catalyst
27 mass. For instance, initial methanol formation rate from Syngas-2 over CZ-H
28 at 250°C and 50 bar was $\sim 11 \mu\text{mol/s/g}_{\text{catal.}}$, creating a methanol pressure in
29 the range of 1-5 bar ($\text{SV}=150\text{-}700 \text{ Ncm}^3/\text{min/g}_{\text{catal.}}$) in the product stream,
30 while methanol dehydration rate over H-ZSM-5 at the same temperature
31 and methanol partial pressure of 1.5 bar was higher than $385 \mu\text{mol/s/g}_{\text{catal.}}$.
32 Therefore, conducting the direct DME synthesis from syngas under methanol-
33 dehydration controlled regime, i.e. applying a hybrid catalyst with an excess
34 methanol synthesis function, to investigate the possible effect of methanol
35 synthesis on H-ZSM-5 deactivation was not possible due to practical rea-
36 sons (limitations regarding reactor volume and flow range of the mass flow
37 controllers). Instead, the acid catalyst was used alone and the methanol
38 synthesis conditions were simulated by using syngas (partial pressure around
39 8.5 bar) as the carrier gas for evaporation and introduction of methanol.
40
41
42
43
44
45
46
47
48
49
50
51
52
53

54 Fig. 8 compares H-ZSM-5 deactivation during methanol dehydration us-
55

1
2
3
4
5
6
7
8 ing carrier gases with different compositions (H_2 and CO contents), under
9 otherwise identical conditions. All gas mixtures contain N_2 and CH_4 , which
10 are used as internal standards for GC analyses. The initial methanol conver-
11 sion level was in the range of 72-77% for all the experiments, and despite the
12 slight differences in the initial activity, the results cannot confirm any effect
13 from the carrier gas composition on activity. The deactivation data shows a
14 higher H-ZSM-5 deactivation rate under carrier gases containing CO and a
15 lower rate for carrier gases containing H_2 , suggesting a positive effect from
16 H_2 and a negative effect from CO on H-ZSM-5 stability. A similar conclusion
17 can be drawn from other sets of experiments where changes in the carrier
18 gas composition during the course of one experiment led to alterations in
19 the catalyst deactivation rate. These observations are in agreement with the
20 experimental results reported by Barbosa et al. [40] and Erena et al. [41],
21 where a higher H_2/CO ratio of the synthesis gas was suggested to restrain
22 the formation of deactivating compounds and deactivation of the CZ/ZSM-5
23 hybrid catalysts. In both studies, deactivation of the hybrid catalysts was
24 linked to deposition of carbonaceous species, which were formed on the acid
25 function of the hybrid (probably through MTH reactions), but deposited on
26 the methanol synthesis catalyst. Erena et al. speculated the reaction of hy-
27 drogen with coke precursors as the origin of the reduced deactivation under
28 higher P_{H_2} [41].

29
30
31
32
33
34
35
36
37
38
39
40
41
42
43
44
45
46
47 During the first few hours of the experiments ($TOS < 10$), different pat-
48 terns of methanol conversion development with TOS were observed under
49 different gas compositions, conveying an impression of a potentially impor-
50 tant effect from H_2/CO ratio of the gas on methanol conversion. However,
51
52
53
54
55

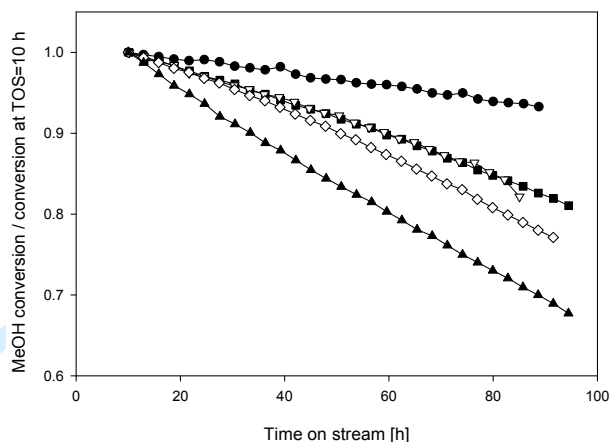


Figure 8: Deactivation of H-ZSM-5 during methanol dehydration to DME using different carrier gases for methanol introduction; Syngas-1 (∇), Syngas-2 (\bullet), CGas-1 (\diamond), CGas-2 (\blacksquare) and CGas-3 (\blacktriangle). $T=250^{\circ}\text{C}$, $P=10$ bar, $X_{\text{MeOH}}=15\%$, $\text{WHSV}=60$ h^{-1} . Methanol conversion is normalized against the conversion at TOS=10 h.

such observations seems highly influenced by unsteady-state conditions at the beginning, and a reliable investigation of these events was limited by the time resolution of the analyses.

CO_2 is only present in small amounts in two of the gases and its possible effect on H-ZSM-5 deactivation cannot be evaluated based on the experiments performed. Methanol dehydration to DME on Lewis acid sites of γ -alumina or ZSM-5 (electron-deficient Al), is known to require adjacent Lewis base sites (electron-rich oxygen bonded to Al) to proceed [68–71]. Similarly, Lewis base sites play an important role in all the proposed methanol dehydration mechanisms on Brønsted acid sites (acidic proton) [72–82]. In theory, the presence of CO_2 as a weak acid can potentially affect methanol dehydration through possible interaction with the basic sites. Such inhibitory effects have been observed from phenol or acetic acid (stronger acids in comparison with

1
2
3
4
5
6
7
8 CO₂) for dehydration of alcohols to ethers on alumina-based catalysts [70].
9
10 Xu et al. [17] claimed that the basic sites of γ -alumina are not sufficiently
11 strong to interact with CO₂ and they confirmed no effect directly from CO₂
12 on methanol dehydration.
13
14

15
16 The effect of CO₂ on deactivation of H-ZSM-5 should also be considered
17 from another perspective. In the presence of Cu-based methanol synthesis
18 catalyst (which also has high water-gas shift activity), the CO₂-content of
19 the synthesis gas is directly linked to the partial pressure of water in the
20 reaction medium. To simulate the effect of CO₂-rich synthesis gas, deionized
21 water was added to liquid methanol feed in the molar ratio of 20/80. This
22 is in the same range as typical water content of the product stream from
23 methanol synthesis unit (crude methanol), i.e. 10-20 mol% water [18]. Fig. 9
24 compares H-ZSM-5 deactivation during methanol dehydration to DME, with
25 and without the presence of water in the feed, under otherwise identical
26 conditions. For the run with water-methanol mixture as feed, a higher liquid
27 flow and a higher total pressure was used to create a similar flow rate and
28 partial pressure of methanol as in the run with dry feed. The role of water
29 in inhibition of the deactivation is apparent from the presented data. These
30 results are consistent with the positive effects reported for a high CO₂ or
31 water content of the feed on stability of hybrid catalysts during direct DME
32 synthesis [20, 83].
33
34
35
36
37
38
39
40
41
42
43
44
45
46

47 It is worth stressing that, despite the positive effect of water on H-ZSM-5
48 stability, water may decrease DME yield, both by reducing catalyst activity
49 through competitive adsorption onto Lewis acid sites (which are not the
50 primary active sites of H-ZSM-5 though), and by enhancing reverse reaction
51
52
53
54
55
56
57
58
59
60

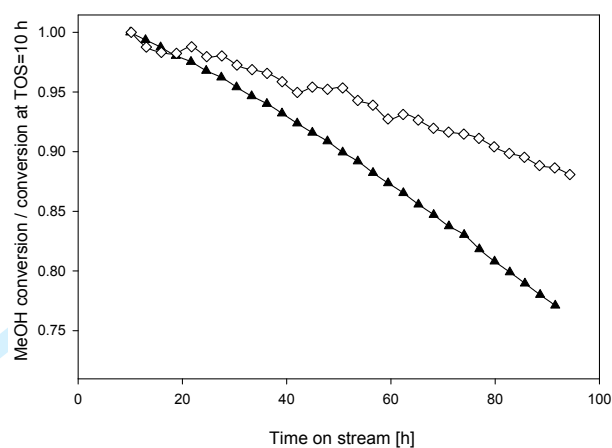


Figure 9: Evolution of methanol conversion to DME over H-ZSM-5 from dry methanol feed (▲) and 19.5 mol% water-in-methanol mixture (◇) with CGas-1 as carrier gas, at 250°C, $P_{\text{MeOH}}=1.5$ bar, $SV=60$ h⁻¹ and $P_{\text{total}}=10$ and 10.4 bar, respectively.

as water is a product of methanol dehydration. With Lewis acid sites as the only active sites, such inhibitory effects are clearly more pronounced for methanol dehydration on $\gamma\text{-Al}_2\text{O}_3$ [17, 20]. For the runs presented in Fig. 9, the initial methanol conversion rate was ~ 350 $\mu\text{mol/s/g}_{\text{catal}}$ in the presence of water as opposed to ~ 385 $\mu\text{mol/s/g}_{\text{catal}}$ from the dry feed.

3.4. Catalyst regeneration

Deactivation of the zeolite catalysts is much slower during methanol dehydration to DME in comparison to conditions with high contact times and large amount of hydrocarbon formation; for which frequent in situ/continuous catalyst regeneration is required. Nevertheless, in the present study, some efforts were directed towards investigating the possibility of H-ZSM-5 regeneration, deactivated during methanol dehydration to DME. Considering the nature of the deactivating hydrocarbons, one potential means of recovering H-

1
2
3
4
5
6
7
8 ZSM-5 activity is in situ thermal treatment of the deactivated catalyst in an
9 inert environment. According to the results of the temperature-programmed
10 desorption analyses presented earlier, deactivating species are expected to de-
11 compose and escape the catalyst below 400°C. As the first attempt, a severely
12 deactivated H-ZSM-5 at 27% of its initial activity was subjected to heating
13 from 250 to 450°C (with the rate of 2°C/min) under N₂ flow, followed by a
14 3 h dwell at 450°C, before being cooled back to 250°C. The gain in activity
15 was ~25%, which is nevertheless only around 3% of the initial activity. A
16 similar procedure with a longer period of heat treatment (14 h) was applied
17 for a less deactivated H-ZSM-5 (80% of the initial activity), and the catalyst
18 activity was recovered to 90% of the initial activity. Such a method, even
19 if efficient for H-ZSM-5, is not applicable for direct DME synthesis catalyst
20 due to the severe thermal deactivation of the methanol synthesis component
21 at such high temperature.
22
23
24
25
26
27
28
29
30
31
32
33

34 Heat treatment in the presence of steam and/or oxygen is a common
35 method for reactivation of the catalysts deactivated by coke [84]. Although
36 coke is not expected to be the main cause of the H-ZSM-5 deactivation during
37 DME production, regeneration of the DME synthesis catalyst through addi-
38 tion of steam or oxygen to the feed has been reported successful by several
39 researchers [20, 58, 83]. Therefore, the usefulness of treatment with steam
40 and O₂ was briefly investigated at temperatures that can be tolerated by
41 the methanol synthesis catalyst. In order to evaluate the effect of water,
42 during the course of methanol dehydration at 250°C and P_{MeOH} of 1.5 bar,
43 1.5 bar steam was added to the reactor on the catalyst severely deactivated
44 to 10% of its initial activity. Steam could not recover the H-ZSM-5 activity
45
46
47
48
49
50
51
52
53
54
55
56
57
58
59
60

1
2
3
4
5
6
7
8 at this temperature, but further deactivation was largely reduced as long as
9 the water was fed. The effect of co-feeding water on reducing deactivation
10 rate of H-ZSM-5 was discussed earlier. Despite our observations, Jun et al.
11 [83] reported a recovery of the H-ZSM-5 activity from ~55% DME yield to
12 almost 80% (initial yield ~90%) by addition of 65 Torr water to the feed
13 (67 Torr methanol) at 250°C.
14
15
16
17
18

19 The last regeneration method examined was controlled oxidation of car-
20 bonaceous compounds of deactivated H-ZSM-5. Such treatment may also
21 be efficient for reactivation of the metallic component of the hybrid cata-
22 lyst deactivated by Cu sintering, through the oxidation-reduction method
23 proposed for redistribution of sintered copper [85–89]. Oxidative treatment
24 of H-ZSM-5 was performed using a partially deactivated catalyst at 55% of
25 its initial activity. The reactor was purged with nitrogen and cooled down
26 to 150°C before air introduction (5%) into the N₂ flow. Subsequently, the
27 reactor was heated up to 250°C with a heating rate of 1°C/min and finally, at
28 250°C, the share of air in the flow was increased gradually to 100% over 1.5 h.
29 Despite the expectations, H-ZSM-5 activity dropped to almost 25% of the
30 initial activity after the treatment. In situ reactivation of hybrid catalysts in
31 diluted oxygen, a CZ/ γ -Al₂O₃ hybrid catalyst at 325°C [58] and a CZ/NaH-
32 ZSM-5 hybrid at 260°C [20], have been reported successful for recovering
33 almost 100% activity even after 10 reaction-regeneration cycles. However, in
34 the both studies, the deactivation was attributed to “coke” formation over
35 the metallic catalyst, while the origin and nature of the deactivating species
36 were not identified clearly. A considerably high selectivity towards paraf-
37 fins (Fischer-Tropsch activity) reported in both studies (which is expected
38
39
40
41
42
43
44
45
46
47
48
49
50
51
52
53
54
55
56
57
58
59
60

1
2
3
4
5
6
7
8 from neither typical methanol synthesis nor acid catalyts) could be a sign
9 of catalyst poisoning with e.g. Fe, and hence, a totally different nature of the
10 deactivating hydrocarbons.
11
12

13 14 15 **4. Conclusion** 16

17
18 The objective of the present work was to investigate the deactivation of
19 hybrid catalysts for direct synthesis of dimethyl ether from synthesis gas. For
20 this, deactivation of both functions of the catalyst, i.e. the methanol synthesis
21 function and the methanol dehydration function, were studied individually,
22 first under their typical corresponding conditions, and then under the con-
23 ditions created by combining both methanol formation and dehydration in
24 a single reactor. In this study, only hybrid catalysts made by physically
25 mixing the pre-pelletized Cu-Zn-based methanol synthesis catalysts and the
26 solid acid catalysts were considered.
27
28

29 Ruling out poisoning, copper sintering was considered as the most likely
30 cause of the methanol synthesis catalysts deactivation. Presence of the solid
31 acid catalysts (zeolite or alumina) showed no additional effect, neither from
32 the catalyst itself nor from the (by)products, on deactivation of the methanol
33 synthesis catalyst. In theory, in situ conversion of synthesized methanol
34 to DME and water could cause a higher partial pressure of water in the
35 reaction medium, assisting copper sintering. However, such an effect cannot
36 be confirmed from our experimental results under the conditions applied.
37
38

39 Accumulation of organic species that are small enough to form inside
40 ZSM-5 cavities, but too large to diffuse out of its channels, is considered as
41 the main cause of ZSM-5 deactivation. Coke formation on the outer surface
42
43
44
45
46
47
48
49
50
51
52
53
54
55
56
57
58
59
60

1
2
3
4
5
6
7
8 of the catalyst may also to a lesser extent contribute to the observed de-
9 activation. Presence of synthesis gas and its composition might have some
10 effects on deactivation of the H-ZSM-5. Presence of H₂ seems to suppress the
11 deactivation while CO appears to enhance it. However, possible effects of im-
12 purities on the observed behavior cannot be excluded completely. Addition
13 of water to the feed for a methanol dehydration experiment, simulating direct
14 DME synthesis from CO₂-rich syngas, is shown to decelerate the deactiva-
15 tion, although at a cost of lower DME yield. Similarly, use of CO₂-deficient
16 syngas for direct DME synthesis is expected to reduce the water content of
17 the reaction medium, assisting ZSM-5 deactivation.
18
19
20
21
22
23
24
25
26
27

28 **Acknowledgment**

29
30 The authors would like to thank Martin F. Sunding at the Center for
31 Material Science and Nanotechnology, the University of Oslo for his help and
32 insights regarding the XPS analyses. The financial support from the Research
33 Council of Norway (contract No. 208351/E30) is gratefully acknowledged.
34
35
36
37
38

39 **References**

- 40
41
42 [1] T. H. Fleisch, A. Basu, R. A. Sills, Introduction and advancement of
43 a new clean global fuel: The status of DME developments in china and
44 beyond, *Journal of Natural Gas Science and Engineering* 9 (2012) 94–
45 107.
46
47
48
49
50 [2] M. Marchionna, R. Patrini, D. Sanfilippo, G. Migliavacca, Fundamental
51 investigations on dimethyl ether (DME) as LPG substitute or make-up
52 for domestic uses, *Fuel Processing Technology* 89 (2008) 1255–1261.
53
54
55

- 1
2
3
4
5
6
7
8 [3] R. Anggarani, C. S. Wibowo, D. Rulianto, Application of dimethyl
9 ether as LPG substitution for household stove, *Energy Procedia* 47
10 (2014) 227–234.
11
12
13
14 [4] C. Arcoumanis, C. Bae, R. Crookes, E. Kinoshita, The potential of
15 dimethyl ether (DME) as an alternative fuel for compression-ignition
16 engines: A review, *Fuel* 87 (2008) 1014–1030.
17
18
19
20 [5] S. H. Park, C. S. Lee, Applicability of dimethyl ether (DME) in a
21 compression ignition engine as an alternative fuel, *Energy Conversion*
22 *and Management* 86 (2014) 848–863.
23
24
25
26 [6] C. Chang, A. Silvestri, Conversion of synthesis gas to gasoline, 1975. US
27 Patent 3,894,102.
28
29
30
31 [7] G. Pagani, Process for the production of dimethyl ether, 1978. US Patent
32 4,098,809.
33
34
35
36 [8] G. C. Chinchin, P. J. Denny, J. R. Jennings, M. S. Spencer, K. C.
37 Waugh, Synthesis of methanol. part 1. catalysts and kinetics, *Applied*
38 *Catalysis* 36 (1988) 1–65.
39
40
41
42 [9] H. H. Kung, Deactivation of methanol synthesis catalysts - a review,
43 *Catalysis Today* 11 (1992) 443–453.
44
45
46
47 [10] M. V. Twigg, M. S. Spencer, Deactivation of supported copper metal
48 catalysts for hydrogenation reactions, *Applied Catalysis A: General* 212
49 (2001) 161–174.
50
51
52
53
54
55
56
57
58
59
60

- 1
2
3
4
5
6
7
8 [11] M. V. Twigg, M. S. Spencer, Deactivation of copper metal catalysts
9 for methanol decomposition, methanol steam reforming and methanol
10 synthesis, *Topics in Catalysis* 22 (2003) 191–203.
11
12
13
14 [12] J. Bøgild-Hansen, P. E. Højlund-Nielsen, Methanol synthesis, in:
15 G. Ertl, H. Knözinger, F. Schüth, J. Weitkamp (Eds.), *Handbook of*
16 *Heterogeneous Catalysis*, Wiley-VCH Verlag GmbH & Co. KGaA, 2008,
17 pp. 2920–2949.
18
19
20
21
22 [13] D. B. Rasmussen, T. V. W. Janssens, B. Temel, T. Bligaard, B. Hinne-
23 mann, S. Helveg, J. Sehested, The energies of formation and mobilities
24 of Cu surface species on Cu and ZnO in methanol and water gas shift
25 atmospheres studied by DFT, *Journal of Catalysis* 293 (2012) 205–214.
26
27
28
29
30
31 [14] G. Prieto, J. Zecevic, H. Friedrich, K. P. de Jong, P. E. de Jongh,
32 Towards stable catalysts by controlling collective properties of supported
33 metal nanoparticles, *Nature Materials* 12 (2013) 34–39.
34
35
36
37 [15] G. Prieto, J. D. Meeldijk, K. P. de Jong, P. E. de Jongh, Interplay
38 between pore size and nanoparticle spatial distribution: Consequences
39 for the stability of CuZn/SiO₂ methanol synthesis catalysts, *Journal of*
40 *Catalysis* 303 (2013) 31–40.
41
42
43
44
45 [16] M. B. Fichtl, D. Schlereth, N. Jacobsen, I. Kasatkin, J. Schumann,
46 M. Behrens, R. Schlogl, O. Hinrichsen, Kinetics of deactivation on
47 Cu/ZnO/Al₂O₃ methanol synthesis catalysts, *Applied Catalysis A: Gen-*
48 *eral* 502 (2015) 262–270.
49
50
51
52
53
54
55
56
57
58
59
60

- 1
2
3
4
5
6
7
8 [17] M. T. Xu, J. H. Lunsford, D. W. Goodman, A. Bhattacharyya, Syn-
9 thesis of dimethyl ether (DME) from methanol over solid-acid catalysts,
10 Applied Catalysis A: General 149 (1997) 289–301.
11
12
13
14 [18] V. Vishwanathan, K. W. Jun, J. W. Kim, H. S. Roh, Vapour phase
15 dehydration of crude methanol to dimethyl ether over Na-modified H-
16 ZSM-5 catalysts, Applied Catalysis A: General 276 (2004) 251–255.
17
18
19
20 [19] F. Raouf, M. Taghizadeh, A. Eliassi, F. Yaripour, Effects of temperature
21 and feed composition on catalytic dehydration of methanol to dimethyl
22 ether over γ -alumina, Fuel 87 (2008) 2967–2971.
23
24
25
26
27 [20] A. T. Aguayo, J. Erena, I. Sierra, M. Olazar, J. Bilbao, Deactivation and
28 regeneration of hybrid catalysts in the single-step synthesis of dimethyl
29 ether from syngas and CO₂, Catalysis Today 106 (2005) 265–270.
30
31
32
33 [21] U. Olsbye, S. Svelle, M. Bjorgen, P. Beato, T. V. W. Janssens,
34 F. Joensen, S. Bordiga, K. P. Lillerud, Conversion of methanol to hydro-
35 carbons: How zeolite cavity and pore size controls product selectivity,
36 Angewandte Chemie-International Edition 51 (2012) 5810–5831.
37
38
39
40 [22] M. Bjorgen, S. Svelle, F. Joensen, J. Nerlov, S. Kolboe, F. Bonino,
41 L. Palumbo, S. Bordiga, U. Olsbye, Conversion of methanol to hy-
42 drocarbons over zeolite HZSM-5: On the origin of the olefinic species,
43 Journal of Catalysis 249 (2007) 195–207.
44
45
46
47
48
49
50 [23] J. Weitkamp, L. Puppe, Catalysis and Zeolites: Fundamentals and Ap-
51 plications, Springer, 1999.
52
53
54
55
56
57
58
59
60

- 1
2
3
4
5
6
7
8 [24] M. Guisnet, F. Ribeiro, Deactivation and Regeneration of Zeolite Cata-
9 lysts, Imperial College Press, 2011.
10
11
12 [25] H. Schulz, D. Barth, Z. Siwei, Deactivation of HZSM-5 zeolite during
13 methanol conversion: Kinetic probing of pore-architecture and acidic
14 properties, in: Studies in Surface Science and Catalysis, volume 68,
15 1991, pp. 783–790.
16
17
18 [26] H. Schulz, Z. Siwei, H. Kusterer, Autocatalysis, retardation, reanimation
19 and deactivation during methanol conversion on zeolite HZSM-5, in:
20 Studies in Surface Science and Catalysis, volume 60, 1991, pp. 281–290.
21
22
23 [27] H. Schulz, K. Lau, M. Claeys, Kinetic regimes of zeolite deactivation
24 and reanimation, Applied Catalysis A: General 132 (1995) 29–40.
25
26
27 [28] H. Schulz, M. Wei, Deactivation and thermal regeneration of zeolite
28 HZSM-5 for methanol conversion at low temperature (260-290°C), Mi-
29 croporous and Mesoporous Materials 29 (1999) 205–218.
30
31
32 [29] H. Schulz, M. Wei, Regimes of methanol conversion on zeolites, in:
33 Studies in Surface Science and Catalysis, volume 154 C, 2004, pp. 2133–
34 2142.
35
36
37 [30] H. Schulz, "coking" of zeolites during methanol conversion: Basic re-
38 actions of the MTO-, MTP- and MTG-processes, Catalysis Today 154
39 (2010) 183–194.
40
41
42 [31] H. Schulz, Time resolved selectivity for unsteady regimes in catalytic
43 petroleum chemistry, Catalysis Today 178 (2011) 151–156.
44
45
46
47
48
49
50
51
52
53
54
55
56
57
58
59
60

- 1
2
3
4
5
6
7
8 [32] H. Schulz, M. Wei, Pools and constraints in methanol conversion to
9 olefins and fuels on zeolite HZSM-5, *Topics in Catalysis* 57 (2014) 683–
10 692.
11
12
13
14 [33] Y. S. Luan, H. Y. Xu, C. Y. Yu, W. Z. Li, S. F. Hou, Effects and control
15 of steam in the systems of methanol and DME synthesis from syngas
16 over cu-based catalysts, *Catalysis Letters* 125 (2008) 271–276.
17
18
19
20 [34] J. Wu, M. Saito, M. Takeuchi, T. Watanabe, The stability of Cu/ZnO-
21 based catalysts in methanol synthesis from a CO₂-rich feed and from a
22 CO-rich feed, *Applied Catalysis A: General* 218 (2001) 235–240.
23
24
25
26 [35] J. T. Sun, I. S. Metcalfe, M. Sahibzada, Deactivation of Cu/ZnO/Al₂O₃
27 methanol synthesis catalyst by sintering, *Industrial & Engineering*
28 *Chemistry Research* 38 (1999) 3868–3872.
29
30
31
32 [36] S. Lee, *Methanol synthesis Thechnology*, CRC Press, Boca Raton,
33 Florida, 1990.
34
35
36
37 [37] V. V. Ordonsky, M. Cai, V. Sushkevich, S. Moldovan, O. Ersen,
38 C. Lancelot, V. Valtchev, A. Y. Khodakov, The role of external acid
39 sites of ZSM-5 in deactivation of hybrid CuZnAl/ZSM-5 catalyst for di-
40 rect dimethyl ether synthesis from syngas, *Applied Catalysis A: General*
41 486 (2014) 266–275.
42
43
44
45
46
47
48 [38] T. Tartamella, S. G. Lee, Role of in-situ produced methanol on the
49 catalyst deactivation in the liquid phase methanol synthesis process,
50 *Fuel Science & Technology International* 14 (1996) 713–727.
51
52
53
54
55
56
57
58
59
60

- 1
2
3
4
5
6
7
8 [39] J. S. Campbell, Influences of catalyst formulation and poisoning on the
9 activity and die-off of low temperature shift catalysts, *Ind. Eng. Chem.,*
10 *Process Des. Develop.* 9 (1970) 588–95.
11
12
13
14 [40] F. S. R. Barbosa, V. S. O. Ruiz, J. L. F. Monteiro, R. R. de Avillez,
15 L. E. P. Borges, L. G. Appel, The deactivation modes of Cu/ZnO/Al₂O₃
16 and HZSM-5 physical mixture in the one-step DME synthesis, *Catalysis*
17 *Letters* 126 (2008) 173–178.
18
19
20
21
22 [41] J. Erena, R. Garona, J. M. Arandes, A. T. Aguayo, J. Bilbao, Effect
23 of operating conditions on the synthesis of dimethyl ether over a CuO-
24 ZnO-Al₂O₃/NaHZSM-5 bifunctional catalyst, *Catalysis Today* 107-08
25 (2005) 467–473.
26
27
28
29
30 [42] X. Peng, B. Toseland, R. Underwood, A novel mechanism of cata-
31 lyst deactivation in liquid phase synthesis gas-to-DME reactions, in:
32 C. Bartholomew, G. Fuentes (Eds.), *Studies in surface science and catal-*
33 *ysis*, volume 111, Elsevier, 1997, pp. 175 – 182.
34
35
36
37
38 [43] A. García-Trenco, A. Vidal-Moya, A. Martínez, Study of the interaction
39 between components in hybrid CuZnAl/HZSM-5 catalysts and its im-
40 pact in the syngas-to-DME reaction, *Catalysis Today* 179 (2012) 43–51.
41
42
43
44 [44] A. García-Trenco, A. Martínez, Direct synthesis of DME from syngas
45 on hybrid CuZnAl/ZSM-5 catalysts: New insights into the role of zeolite
46 acidity, *Applied Catalysis A: General* 411 (2012) 170–179.
47
48
49
50 [45] A. García-Trenco, A. Martínez, The influence of zeolite surface-
51
52
53
54
55
56
57
58
59
60

- 1
2
3
4
5
6
7
8 aluminum species on the deactivation of CuZnAl/zeolite hybrid catalysts
9 for the direct DME synthesis, *Catalysis Today* 227 (2013) 144–153.
- 10
11
12 [46] A. García-Trenco, S. Valencia, A. Martínez, The impact of zeolite pore
13 structure on the catalytic behavior of CuZnAl/zeolite hybrid catalysts
14 for the direct DME synthesis, *Applied Catalysis A: General* 468 (2013)
15 102–111.
- 16
17
18 [47] A. García-Trenco, A. Martínez, A rational strategy for preparing Cu-
19 ZnO/H-ZSM-5 hybrid catalysts with enhanced stability during the one-
20 step conversion of syngas to dimethyl ether (DME), *Applied Catalysis*
21 *A: General* 493 (2015) 40–49.
- 22
23
24 [48] H. Bakhtiary-Davijany, F. Dadgar, F. Hayer, X. K. Phan, R. Myrstad,
25 H. J. Venvik, P. Pfeifer, A. Holmen, Analysis of external and internal
26 mass transfer at low reynolds numbers in a multiple-slit packed bed mi-
27 crostructured reactor for synthesis of methanol from syngas, *Industrial*
28 *& Engineering Chemistry Research* 51 (2012) 13574–13579.
- 29
30
31 [49] H. Bakhtiary-Davijany, F. Hayer, X. K. Phan, R. Myrstad, P. Pfeifer,
32 H. J. Venvik, A. Holmen, Performance of a multi-slit packed bed mi-
33 crostructured reactor in the synthesis of methanol: Comparison with a
34 laboratory fixed-bed reactor, *Chemical Engineering Science* 66 (2011)
35 6350–6357.
- 36
37
38 [50] H. Bakhtiary-Davijany, F. Hayer, X. K. Phan, R. Myrstad, H. J. Venvik,
39 P. Pfeifer, A. Holmen, Characteristics of an integrated micro packed bed
40
41
42
43
44
45
46
47
48
49
50
51
52
53
54
55
56
57
58
59
60

- 1
2
3
4
5
6
7
8 reactor-heat exchanger for methanol synthesis from syngas, *Chemical*
9 *Engineering Journal* 167 (2011) 496–503.
- 10
11
12 [51] F. Hayer, H. Bakhtiary-Davijany, R. Myrstad, A. Holmen, P. Pfeifer,
13 H. J. Venvik, Characteristics of integrated micro packed bed reactor-
14 heat exchanger configurations in the direct synthesis of dimethyl ether,
15 *Chemical Engineering and Processing: Process Intensification* 70 (2013)
16 77–85.
- 17
18 [52] F. Hayer, H. Bakhtiary-Davijany, R. Myrstad, A. Holmen, P. Pfeifer,
19 H. J. Venvik, Synthesis of dimethyl ether from syngas in a microchan-
20 nel reactor: Simulation and experimental study, *Chemical Engineering*
21 *Journal* 167 (2011) 610–615.
- 22
23 [53] F. Hayer, H. Bakhtiary-Davijany, R. Myrstad, A. Holmen, P. Pfeifer,
24 H. J. Venvik, Modeling and simulation of an integrated micro packed bed
25 reactor-heat exchanger configuration for direct dimethyl ether synthesis,
26 *Topics in Catalysis* 54 (2011) 817–827.
- 27
28 [54] R. Myrstad, S. Eri, P. Pfeifer, E. Rytter, A. Holmen, Fischer-tropsch
29 synthesis in a microstructured reactor, *Catalysis Today* 147 (2009) S301–
30 S304.
- 31
32 [55] J. Erena, I. Sierra, M. Azar, A. G. Gayubo, A. T. Aguayo, Deactiva-
33 tion of a CuO-ZnO-Al₂O₃/γ-Al₂O₃ catalyst in the synthesis of dimethyl
34 ether, *Industrial & Engineering Chemistry Research* 47 (2008) 2238–
35 2247.
- 36
37
38
39
40
41
42
43
44
45
46
47
48
49
50
51
52
53
54
55
56
57
58
59
60

- 1
2
3
4
5
6
7
8 [56] I. Sierra, J. Erena, A. T. Aguayo, M. Olazar, J. Bilbao, Deactivation ki-
9 netics for direct dimethyl ether synthesis on a CuO-ZnO-Al₂O₃/γ-Al₂O₃
10 catalyst, *Industrial and Engineering Chemistry Research* 49 (2010) 481–
11 489.
12
13
14
15
16 [57] I. Sierra, J. Erena, A. T. Aguayo, J. M. Arandes, M. Olazar, J. Bil-
17 bao, Co-feeding water to attenuate deactivation of the catalyst metallic
18 function (CuO-ZnO-Al₂O₃) by coke in the direct synthesis of dimethyl
19 ether, *Applied Catalysis B: Environmental* 106 (2011) 167–173.
20
21
22 [58] I. Sierra, J. Erena, A. T. Aguayo, J. M. Arandes, J. Bilbao, Regeneration
23 of CuO-ZnO-Al₂O₃/γ-Al₂O₃ catalyst in the direct synthesis of dimethyl
24 ether, *Applied Catalysis B: Environmental* 94 (2010) 108–116.
25
26
27 [59] F. Huber, Z. X. Yu, S. Logdberg, M. Ronning, D. Chen, H. Venvik,
28 A. Holmen, Remarks on the passivation of reduced Cu-, Ni-, Fe-, Co-
29 based catalysts, *Catalysis Letters* 110 (2006) 211–220.
30
31
32 [60] M. Sahibzada, I. S. Metcalfe, D. Chadwick, Methanol synthesis from
33 CO/CO₂/H₂ over Cu/ZnO/Al₂O₃ at differential and finite conversions,
34 *Journal of Catalysis* 174 (1998) 111–118.
35
36
37 [61] C. Kuechen, U. Hoffmann, Investigation of simultaneous reaction of
38 carbon-monoxide and carbon-dioxide with hydrogen on a commercial
39 copper-zinc oxide catalyst, *Chemical Engineering Science* 48 (1993)
40 3767–3776.
41
42
43 [62] K. C. Waugh, Methanol synthesis, *Catalysis Letters* 142 (2012) 1153–
44 1166.
45
46
47
48
49
50
51
52
53
54
55
56
57
58
59
60

- 1
2
3
4
5
6
7
8 [63] P. L. Hansen, J. B. Wagner, S. Helveg, J. R. Rostrup-Nielsen, B. S.
9 Clausen, H. Topsoe, Atom-resolved imaging of dynamic shape changes
10 in supported copper nanocrystals, *Science* 295 (2002) 2053–2055.
11
12
13
14 [64] G. A. Vedage, R. Pitchai, R. G. Herman, K. Klier, Water promotion and
15 identification of intermediates in methanol synthesis, in: *Proceedings,*
16 *8th International Congress on Catalysis, volume II, 1984, pp. 47–59.*
17
18
19
20 [65] S. Jiang, J. S. Hwang, T. H. Jin, T. X. Cai, W. Cho, Y. S. Baek, S. E.
21 Park, Dehydration of methanol to dimethyl ether over ZSM-5 zeolite,
22 *Bulletin of the Korean Chemical Society* 25 (2004) 185–189.
23
24
25
26 [66] W. G. Song, D. M. Marcus, H. Fu, J. O. Ehresmann, J. F. Haw, An oft-
27 studied reaction that may never have been: Direct catalytic conversion
28 of methanol or dimethyl ether to hydrocarbons on the solid acids HZSM-
29 5 or HSAPO-34, *Journal of the American Chemical Society* 124 (2002)
30 3844–3845.
31
32
33
34 [67] F. Dadgar, R. Myrstad, P. Pfeifer, A. Holmen, H. J. Venvik, Direct
35 dimethyl ether synthesis from synthesis gas: The influence of methanol
36 dehydration on methanol synthesis reaction, *Catalysis Today* (2015).
37
38
39
40 [68] N. S. Figoli, S. A. Hillar, J. M. Parera, Poisoning and nature of alumina
41 surface in dehydration of methanol, *Journal of Catalysis* 20 (1971) 230–
42 237.
43
44
45
46 [69] H. Pines, J. Manassen, *The Mechanism of Dehydration of Alcohols over*
47 *Alumina Catalysts, volume Volume 16, Academic Press, 1966, pp. 49–*
48 *93.*
49
50
51
52
53
54
55
56
57
58
59
60

- 1
2
3
4
5
6
7
8 [70] J. R. Jain, C. N. Pillai, Catalytic dehydration of alcohols over alumina
9 mechanism of ether formation, *Journal of Catalysis* 9 (1967) 322–330.
10
11
12 [71] R. S. Schifano, R. P. Merrill, A mechanistic study of the methanol
13 dehydration reaction on gamma-alumina catalyst, *Journal of Physical*
14 *Chemistry* 97 (1993) 6425–6435.
15
16
17 [72] Y. Ono, T. Mori, Mechanism of methanol conversion into hydrocarbons
18 over ZSM-5 zeolite, *Journal of the Chemical Society-Faraday Transac-*
19 *tions I* 77 (1981) 2209–2221.
20
21
22 [73] T. R. Forester, R. F. Howe, Insitu ftir studies of methanol and dimethyl
23 ether in ZSM-5, *Journal of the American Chemical Society* 109 (1987)
24 5076–5082.
25
26
27 [74] J. G. Highfield, J. B. Moffat, Elucidation of the mechanism of de-
28 hydration of methanol over 12-tungstophosphoric acid using infrared
29 photoacoustic-spectroscopy, *Journal of Catalysis* 95 (1985) 108–119.
30
31
32 [75] Z. Qinwei, D. Jingfa, Studies on the properties of water in and conversion
33 of methanol into dimethyl ether on $H_3PW_{12}O_{40}$, *Journal of Catalysis*
34 116 (1989) 298–302.
35
36
37 [76] L. Kubelkova, J. Novakova, K. Nedomova, Reactivity of surface species
38 on zeolites in methanol conversion, *Journal of Catalysis* 124 (1990) 441–
39 450.
40
41
42 [77] W. Z. Lu, L. H. Teng, W. D. Xiao, Simulation and experiment study of
43 dimethyl ether synthesis from syngas in a fluidized-bed reactor, *Chem-*
44 *ical Engineering Science* 59 (2004) 5455–5464.
45
46
47
48
49
50
51
52
53
54
55
56
57
58
59
60

- 1
2
3
4
5
6
7
8 [78] J. Bandiera, C. Naccache, Kinetics of methanol dehydration on dealumi-
9 nated H-mordenite - model with acid and basic active-centers, *Applied*
10 *Catalysis* 69 (1991) 139–148.
11
12
13
14 [79] K. S. Ha, Y. J. Lee, J. W. Bae, Y. W. Kim, M. H. Woo, H. S. Kim,
15 M. J. Park, K. W. Jun, New reaction pathways and kinetic parame-
16 ter estimation for methanol dehydration over modified ZSM-5 catalysts,
17 *Applied Catalysis A: General* 395 (2011) 95–106.
18
19
20
21
22 [80] S. R. Blaszowski, R. A. van Santen, The mechanism of dimethyl ether
23 formation from methanol catalyzed by zeolitic protons, *Journal of the*
24 *American Chemical Society* 118 (1996) 5152–5153.
25
26
27
28 [81] S. R. Blaszowski, R. A. van Santen, Theoretical study of the mecha-
29 nism of surface methoxy and dimethyl ether formation from methanol
30 catalyzed by zeolitic protons, *Journal of Physical Chemistry B* 101
31 (1997) 2292–2305.
32
33
34
35
36 [82] R. T. Carr, M. Neurock, E. Iglesia, Catalytic consequences of acid
37 strength in the conversion of methanol to dimethyl ether, *Journal of*
38 *Catalysis* 278 (2011) 78–93.
39
40
41
42
43 [83] K. W. Jun, H. S. Lee, H. S. Roh, S. E. Park, Highly water-enhanced H-
44 ZSM-5 catalysts for dehydration of methanol to dimethyl ether, *Bulletin*
45 *of the Korean Chemical Society* 24 (2003) 106–108.
46
47
48
49 [84] D. L. Trimm, *Deactivation and Regeneration*, Wiley-VCH Verlag
50 GmbH, 2008, pp. 1263–1282.
51
52
53
54
55
56
57
58
59
60

- 1
2
3
4
5
6
7
8 [85] W. Cheng, Regeneration of methanol dissociation catalysts, 8 Aug, 1989.
9 US Patent 4,855,267.
10
11
12 [86] S. Lee, S. Ashok, C. Kulik, Process for in-situ regeneration of aged
13 methanol catalysts, April 2, 1991. US Patent 5,004,717.
14
15
16
17 [87] B. G. Lee, S. Lee, C. J. Kulik, Regeneration of liquid-phase methanol
18 synthesis catalyst, Fuel Sci. Technol. Int. 9 (1991) 587–612.
19
20
21 [88] S. G. Lee, A. Sardesai, Liquid phase methanol and dimethyl ether syn-
22 thesis from syngas, Topics in Catalysis 32 (2005) 197–207.
23
24
25
26 [89] Y. S. Luan, H. Y. Xu, C. Y. Yu, W. Z. Li, S. F. Hou, In-situ regeneration
27 mechanisms of hybrid catalysts in the one-step synthesis of dimethyl
28 ether from syngas, Catalysis Letters 115 (2007) 23–26.
29
30
31
32
33
34
35
36
37
38
39
40
41
42
43
44
45
46
47
48
49
50
51
52
53
54
55
56
57
58
59
60

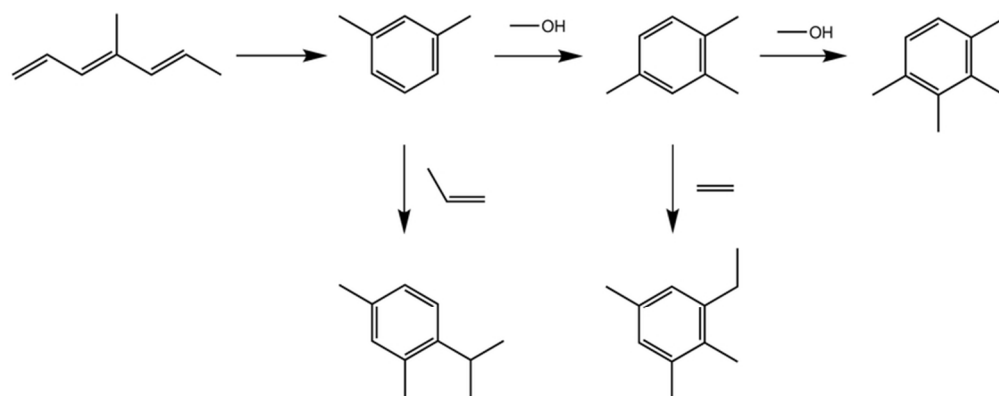


Figure 1

72x28mm (300 x 300 DPI)

Peer Review

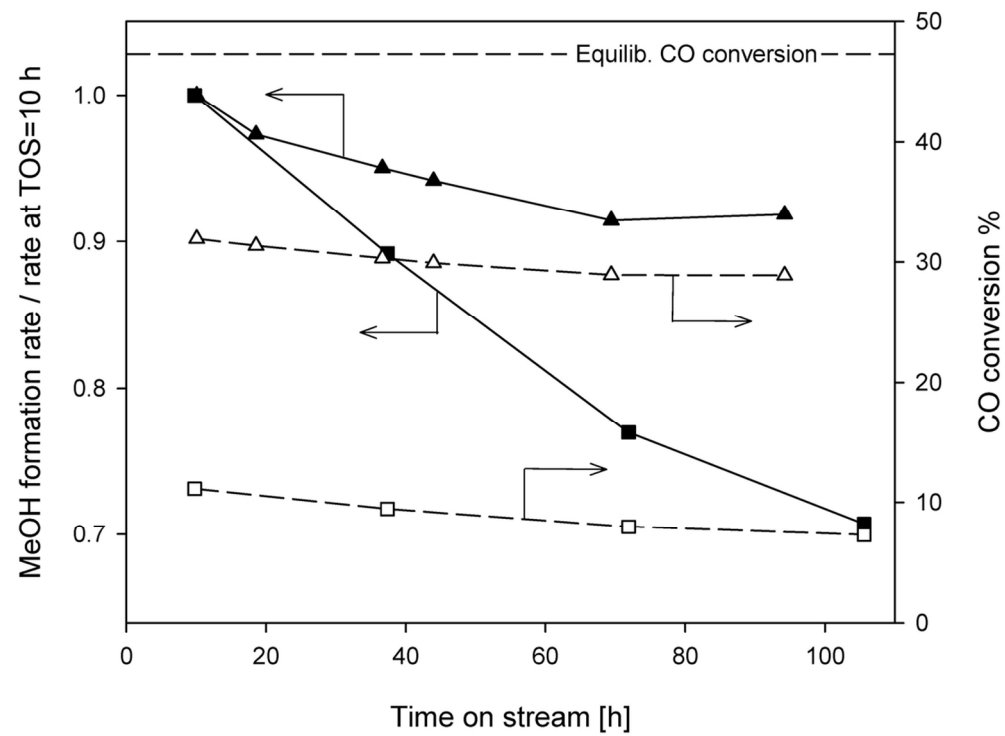


Figure 2

108x80mm (300 x 300 DPI)

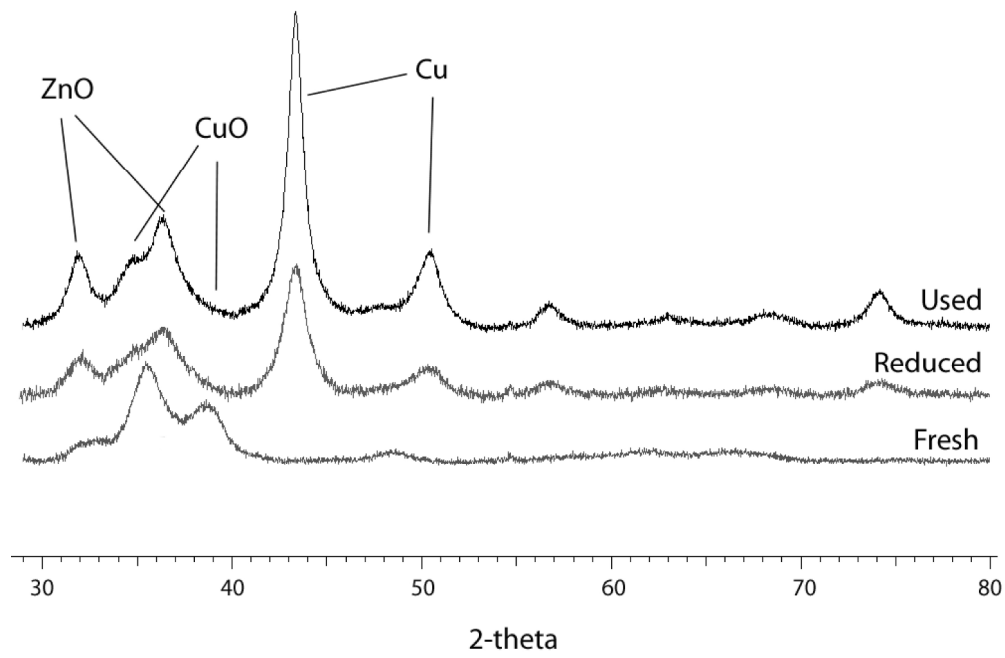


Figure 3

242x165mm (300 x 300 DPI)

1
2
3
4
5
6
7
8
9
10
11
12
13
14
15
16
17
18
19
20
21
22
23
24
25
26
27
28
29
30
31
32
33
34
35
36
37
38
39
40
41
42
43
44
45
46
47
48
49
50
51
52
53
54
55
56
57
58
59
60

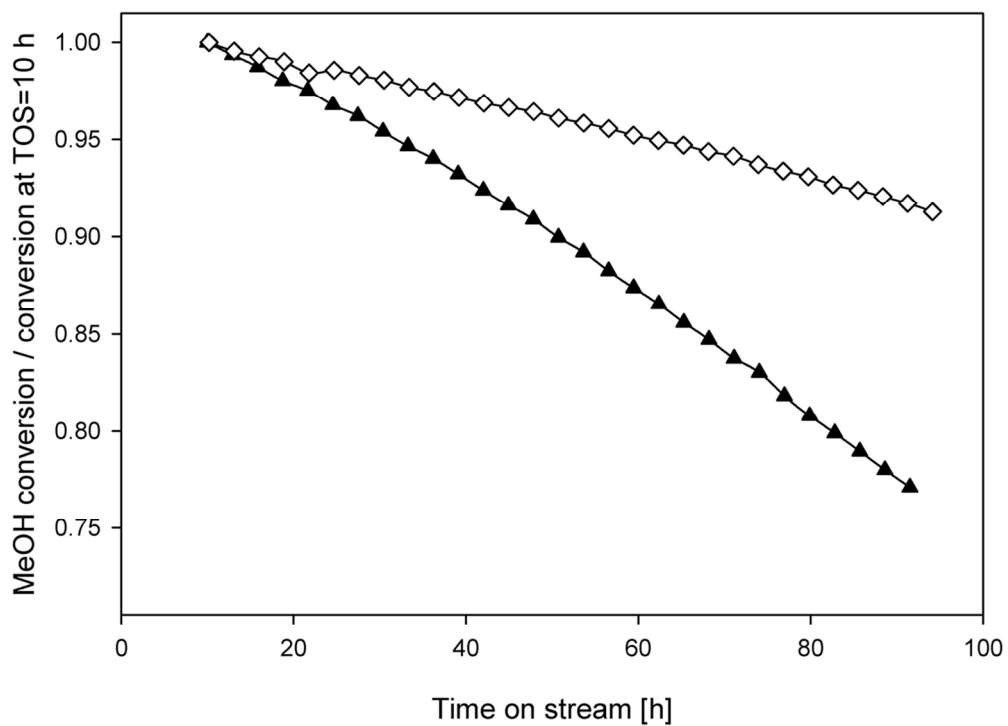


Figure 4

108x80mm (300 x 300 DPI)

Review

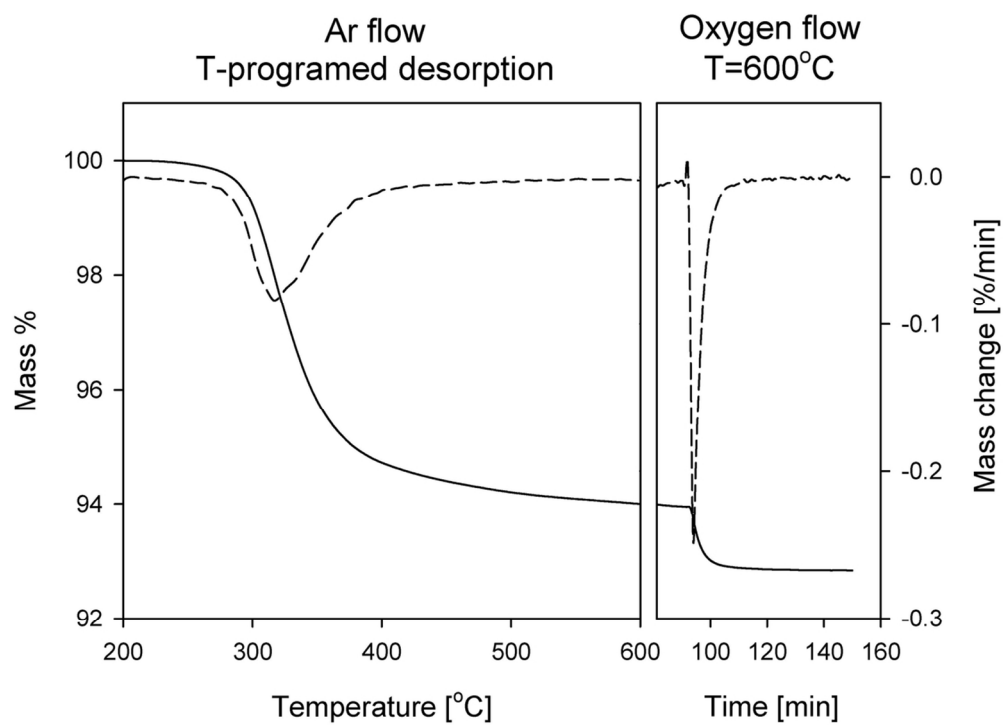


Figure 5

108x80mm (300 x 300 DPI)

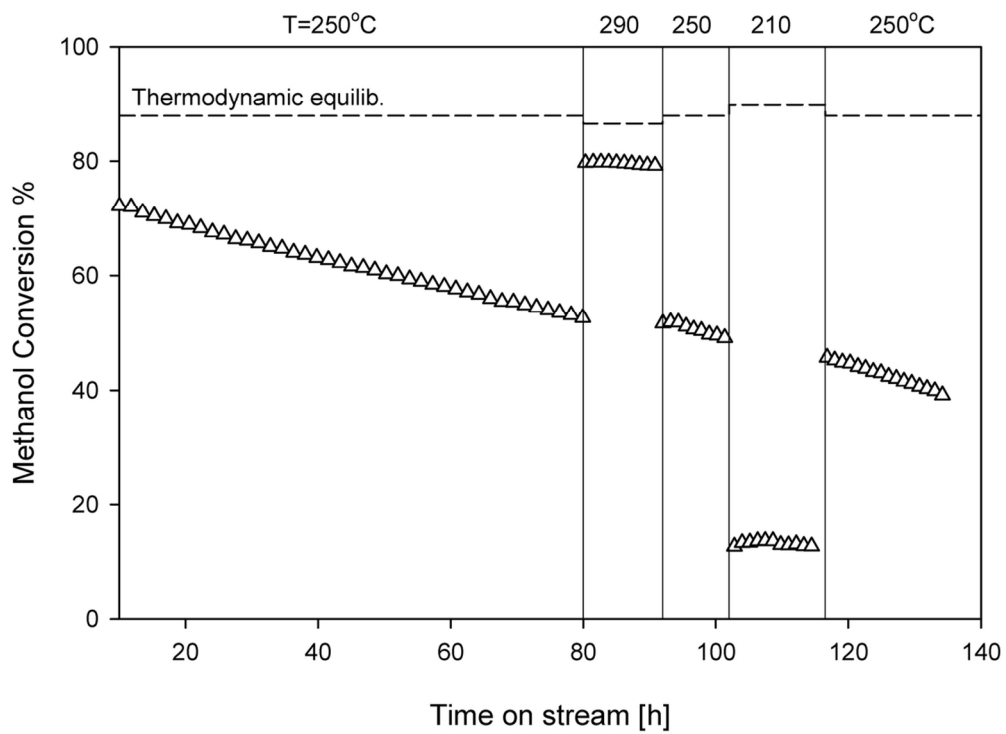


Figure 6

108x80mm (300 x 300 DPI)

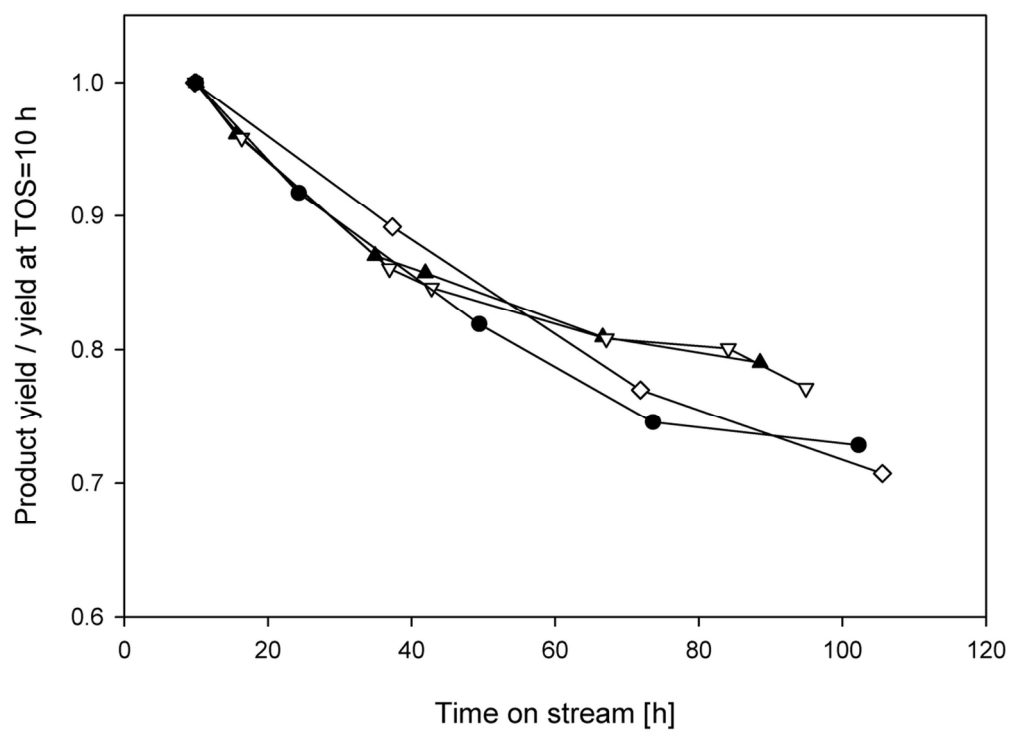


Figure 7

108x80mm (300 x 300 DPI)

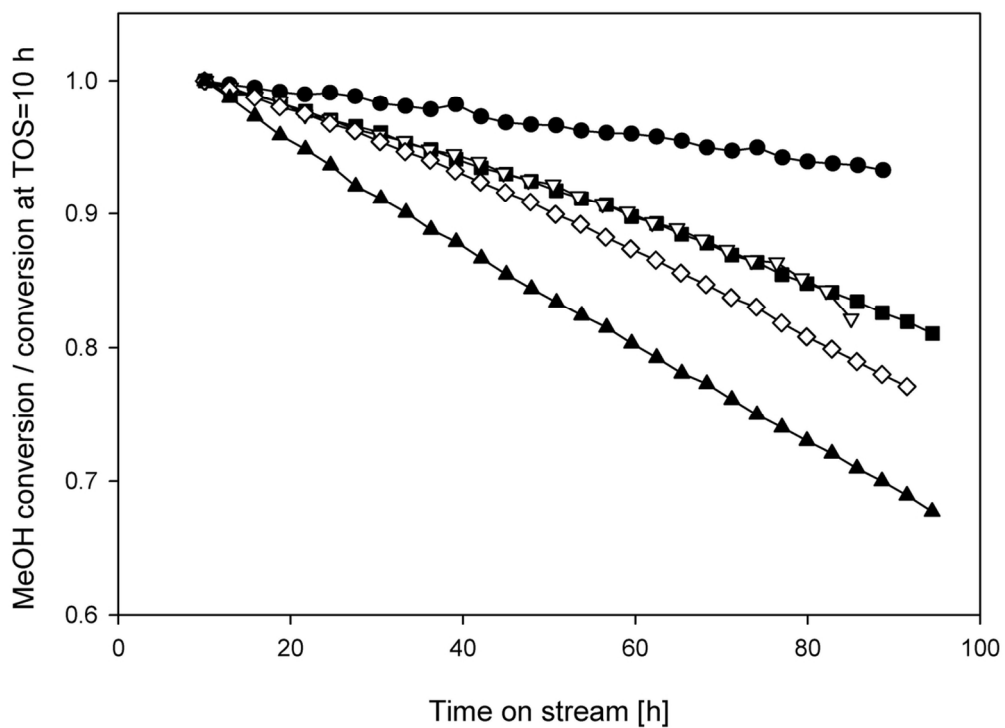


Figure 8

108x80mm (300 x 300 DPI)

Review

1
2
3
4
5
6
7
8
9
10
11
12
13
14
15
16
17
18
19
20
21
22
23
24
25
26
27
28
29
30
31
32
33
34
35
36
37
38
39
40
41
42
43
44
45
46
47
48
49
50
51
52
53
54
55
56
57
58
59
60

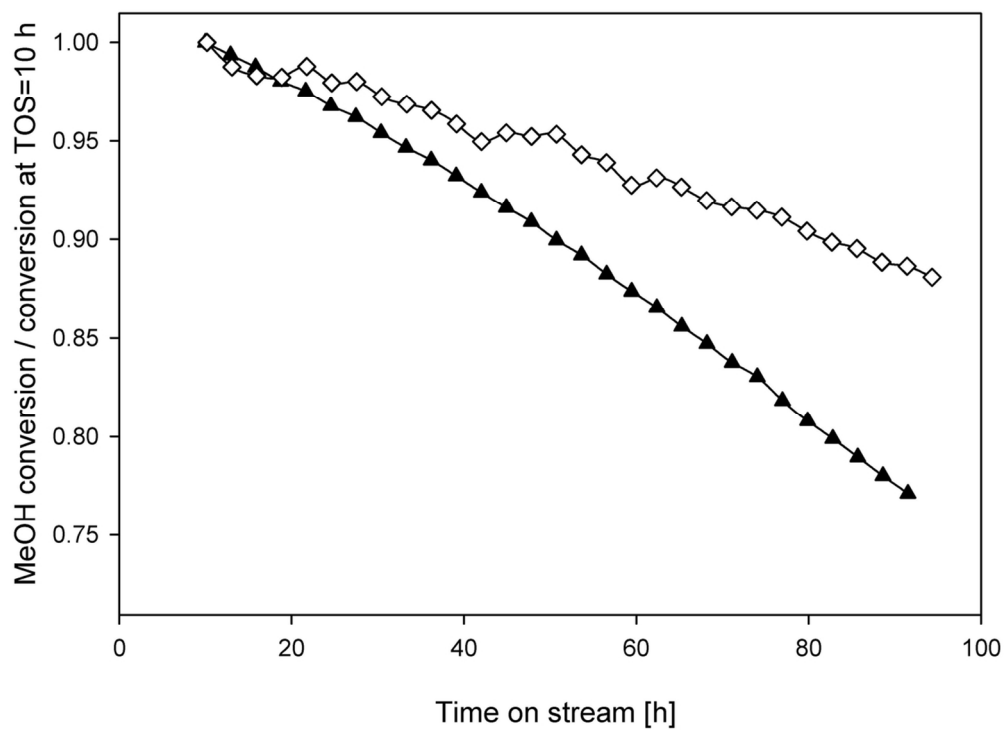


Figure 9

108x80mm (300 x 300 DPI)